AGU PUBLICATIONS

JGR

Journal of Geophysical Research: Planets

RESEARCH ARTICLE
10.1002/2013JE004505

Key Points:
- A mantle-atmosphere coupled model of Venus is investigated using volatile fluxes
- Realistic Venus-like behavior is obtained for the mantle and atmosphere
- Feedback from surface conditions can have strong effects on mantle dynamics

Correspondence to:
C. Gillmann,
cedric.gillmann@observatoire.be

Citation:
Gillmann, C., and P. Tackley (2014), Atmosphere/mantle coupling and feedbacks on Venus, *J. Geophys. Res. Planets*, *119*, doi:10.1002/2013JE004505.

Received 19 AUG 2013
Accepted 23 APR 2014
Accepted article online 29 APR 2014

Atmosphere/mantle coupling and feedbacks on Venus

Cedric Gillmann[1,2] and Paul Tackley[1]

[1]Department of Earth Sciences, ETH Zürich, Institute of Geophysics, Zürich, Switzerland, [2]Now at Royal Observatory of Belgium, Brussels, Belgium

Abstract We investigate the coupled evolution of the atmosphere and mantle on Venus. Here we focus on mechanisms that deplete or replenish the atmosphere: atmospheric escape to space and volcanic degassing of the mantle. These processes are linked to obtain a coupled model of mantle convection and atmospheric evolution, including feedback of the atmosphere on the mantle via the surface temperature. During early atmospheric evolution, hydrodynamic escape is dominant, while for later evolution we focus on nonthermal escape, as observed by the Analyzer of Space Plasma and Energetic Atoms instrument on the Venus Express Mission. The atmosphere is replenished by volcanic degassing from the mantle, using mantle convection simulations based on those of *Armann and Tackley* [2012], and include episodic lithospheric overturn. The evolving surface temperature is calculated from the amount of CO_2 and water in the atmosphere using a gray radiative-convective atmosphere model. This surface temperature in turn acts as a boundary condition for the mantle convection model. We obtain a Venus-like behavior (episodic lid) for the solid planet and an atmospheric evolution leading to the present conditions. CO_2 pressure is unlikely to vary much over the history of the planet, with only a 0.25–20% postmagma-ocean buildup. In contrast, atmospheric water vapor pressure is strongly sensitive to volcanic activity, leading to variations in surface temperatures of up to 200 K, which have an effect on volcanic activity and mantle convection. Low surface temperatures trigger a mobile lid regime that stops once surface temperatures rise again, making way to stagnant lid convection that insulates the mantle.

1. Introduction and Goals

A good way to study habitability is to compare the one planet known to shelter life with other similar planets that do not (as far as we know), which are presently Mars and Venus. Extrasolar super-Earths are being discovered, and the first observations of them (other than size and mass) will be of their atmospheres, further motivating the goal of understanding atmosphere-interior coupling. Taking our solar system as a pattern, CO_2 atmospheres are likely to be common. Venus is the planet that is the most similar to Earth in size, but it exhibits much different climate and behavior, making it an ideal choice for studying possible causes of the divergent evolution of planets.

Venus has similar general characteristics to Earth. It has roughly the same size (slightly smaller) and is thought to have formed in the same way with the same basic components. It has an atmosphere, climatic system, and greenhouse effect. Conditions at its surface are, however, far from those on Earth's surface. The average surface temperature of Venus is around 740 K due to the strong greenhouse effect of its 92 bar atmosphere, which is mainly composed of CO_2 but contains 30 ppm water [*de Bergh et al.*, 1995; *Taylor and Grinspoon*, 2009]; no liquid water exists. Clouds composed of sulfuric acid can be found in its atmosphere [*Esposito et al.*, 1983].

The solid part of the planet is still active, as evidenced both by indirect clues [*Grinspoon*, 1993; *Bullock and Grinspoon*, 2001; *Fegley and Prinn*, 1989] and by direct recent observations [*Smrekar et al.*, 2010; *Shaligyn et al.*, 2014]. Additionally, it is generally thought that, based on crater counting, the surface of Venus is relatively young and with a quite uniform surface age of 300 Myr to 1 Gyr [*McKinnon et al.*, 1997; *Schaber et al.*, 1992; *Strom et al.*, 1994]. A common interpretation of this peculiar situation is that Venus has been subjected to a large-scale catastrophic resurfacing event late in its history, which covered much of its ancient surface with younger volcanic material [e.g., *Romeo and Turcotte*, 2010]. This interpretation is often coupled with subsequent low-level volcanic activity during the quiescent phase following the resurfacing

event [*Schaber et al*., 1992; *Strom et al*., 1994; *Turcotte*, 1993; *Phillips et al*., 1992; and first quantified by *Bullock et al*., 1993a, 1993b]. Episodic behavior has also been suggested, but we would only be able to see the effects of the last event.

Such characteristics are directly linked to convection in Venus' mantle. It has been hypothesized that Venus used to have plate tectonics [*Moresi and Solomatov*, 1998; *Schubert et al*., 1997, 2001] before it entered its current stagnant lid regime [*Schubert et al*., 1997; *Nimmo and McKenzie*, 1998]. Episodic plate tectonics featuring global lithospheric overturn events is another possibility [*Schubert et al*., 1997; *Fowler and O'Brian*, 1996; *Turcotte et al*., 1999]. Recently, *Armann and Tackley* [2012] showed using numerical models that episodic lithospheric overturn could be caused by plastic yielding in its lithosphere, which allows "breaking" of the lid. Their episodic lid results displayed a realistic crustal thickness and present-day magmatic rate. In contrast, their results for stagnant lid convection displayed a very thick crust (~150 km) and a very much higher volcanic rate than is currently observed, because magmatic heat pipe was the main heat loss mechanism of the planet.

On an active planet, strong volcanism has a direct influence on the evolution of its atmosphere. Volcanic degassing releases volatiles into the atmosphere. This interaction between the solid planet and its atmosphere is the most obvious and commonly considered one (in the case of Venus by *Bullock and Grinspoon* [1996, 2001], *Phillips and Hansen* [1998], *Zolotov and Volkov* [1992], and *Zolotov* [1996]).

The possibility that the atmosphere could have an influence on the convective regime and solid planet behavior has received less attention. Earlier papers have attempted to deal with this, applying the idea to surface features [*Solomon et al*., 1999; *Anderson and Smrekar*, 1999; *Gerya*, 2014] or to the convective regime [*Lenardic et al*., 2008]. These studies underlined the importance that 50–100 K surface temperature variations could have on the solid planet. *Lenardic et al*. [2008], in particular, showed that temperature variations could modify the convective mode, with high surface temperatures favoring stagnant lid and lower surface temperatures favoring mobile lid.

Studies considering a full two-way coupling of atmosphere and mantle dynamics are comparatively few. *Phillips et al*. [2001] used a parameterized mantle model and a simple gray radiative-convective atmospheric model, finding that surface temperature can have a significant effect on mantle convection and volcanic activity. The authors observed a positive feedback between the greenhouse effect and melting, leading to further destabilization of the climate of the planet. Their study indicated a clear interdependence of climate and mantle convection on Venus. However, the limited nature of the parameterized representation of the mantle prevents a realistic interpretation of the precise effects of the feedback.

On the other hand, *Noack et al*. [2012] used a spherical convection code including melting (GAIA) *Hüttig and Stemmer* [2008] as well as results taken from modeling of Venus' atmosphere by *Bullock and Grinspoon* [2001]. They observed that the greenhouse effect can increase surface temperature to a critical value at which the surface is mobilized, which increases the cooling rate of the mantle and reduces degassing. This results in decreasing concentrations of water in the atmosphere hence lower surface temperatures, thus providing a negative feedback stabilizing mechanism for the climate of Venus.

In the present study we follow a similar approach, coupling atmospheric evolution and mantle convection in a straightforward way through changes in surface conditions. Such an approach is based on the tracking of volatiles through the atmosphere and solid planet system. Therefore, we need to investigate the evolution of volatile fluxes entering and exiting the atmosphere as well as the convective regime of the mantle.

The main processes of interest for the atmosphere are escape (to space) and degassing (of the mantle). Below, we first detail our treatment of atmospheric processes starting with the modeling of hydrodynamic escape, the most primitive mechanism; then, we present how we calculate nonthermal losses, which are dominant at the present day and can be constrained by observations from the ASPERA (Analyzer of Space Plasma and Energetic Atoms) instrument. We also explain the modeling of surface temperature evolution due to the greenhouse effect using a gray radiative-convective atmospheric model and providing a boundary condition for mantle convection. Finally, we focus on the mantle convection simulation using the StagYY planetary mantle convection code [*Tackley*, 2008], and how it generates degassing.

The aim of this work is to test the coupling of different models previously designed for separate operation. We also want to assess the effect of surface temperature on the mantle convection regime and, more

generally, if and how a feedback really occurs. Finally, we want to use available observations both for the solid planet (recent volcanic production rates, age of surface, and heat loss) and present-day atmosphere (present-day total pressure and water concentration as well as escape rates and isotopic fractionation) to constrain our models. We aim to identify possible realistic scenarios for the evolution of Venus given the limitations of the model and available data.

Due to these goals and to the large number of parameters involved in simulations of this scope, however, it is infeasible to run a full search over the full range of all parameters. Thus, in this initial study, we focus on the variation of atmospheric parameters, limiting the mantle physical parameters to a narrow range corresponding to the preferred models in *Armann and Tackley* [2012].

2. Model

Our model for the evolution of Venus is composed of different components that represent the different aspects of the history of the planet. These are focused on volatile exchanges, as they appear to be the main drive for coupling. The coupling is two way. Mantle activity leads to degassing, releasing volatiles into the atmosphere and contributing to the greenhouse effect. On the other hand, the greenhouse effect governs the surface temperature, which acts as a boundary condition for mantle convection.

2.1. Hydrodynamic Escape

Our model for hydrodynamic escape uses part of our past work described in more detail in *Gillmann et al*. [2009]. It is based on an energy-limited calculation of the linked escape of H and O in a water-rich atmosphere subjected to intense primitive extreme UV flux from the Sun. Water is photodissociated into H and O. It is based on previous work by *Zahnle and Kasting*, 1986, *Kasting and Pollack* [1983], *Hunten et al*. [1987], and *Chassefière* [1996a, 1996b]. Following *Kasting and Pollack* [1983] and *Tian et al*. [2008], we use 200 km as the base of the escape where H and O species are dominant and assume that atmospheric temperature is constant between 120 km and 200 km (which is consistent with our simple, simulated atmospheric profiles; see later). We also neglect escape limitation by diffusion.

We focus on the case where H and O have a linked escape and use the same layout and equations as detailed in *Gillmann et al*. [2009], as it has generated more realistic results and total escape rates than the alternative (escape of H unlimited by O). Therefore, hydrodynamic escape is slowed by the heavier species (O) during the first 500 Myr. Later escape only concerns hydrogen, as energy from the Sun (EUV flux) becomes insufficient to enable oxygen to be dragged along with hydrogen. According to our previous results and since the convection code cannot yet model a magma ocean, we focus on the post 100 Myr escape and evolution. By that stage the magma ocean should have crystallized. Indeed, other terrestrial planets (Mars and the Earth) are likely to have had a magma ocean during their first 100 Myr or so [*Debaille et al*., 2007; *Elkins-Tanton*, 2008]. Without a thick atmosphere, a magma ocean would freeze on a timescale of around 10 Myr. Intense escape has been suggested to be able to lead to large decrease in surface temperature during the first 100 Myr of the planet's evolution [*Gillmann et al*., 2009], thus putting an end to the magma ocean phase quite early.

Parameters used here are in line with the best fit from our previous work. Therefore, we take a global efficiency factor of 2.4. This efficiency factor is the ratio of energy made available for escape over solar EUV flux. It includes the efficiency of energy transfer to the upper atmosphere as well as an additional contribution from solar wind and atmospheric expansion, meaning that it can be greater than 1. We also use an escape starting 10 Myr after the beginning of the accretion (the time when the planet first received large amounts of water) and an exosphere temperature of 500 K to 1250 K. Note that escape during the 10–100 Myr period is calculated only for the isotopic fractionation; it is not directly used in the results shown in this study. These values produce the consistent evolution proposed in *Gillmann et al*. [2009] and fit stable isotope fractionation data for Ar and Ne. Reasonable assumptions lead to an estimated escape of several (typically 2–8) terrestrial ocean equivalents during the hydrodynamic phase, with the bulk of the loss occurring during the first 100 Myr.

2.2. Nonthermal Atmospheric Escape

Atmospheric escape is the main way that volatiles are removed from the atmosphere of Venus, and, after hydrodynamic escape has stopped being significant for species heavier than H (500 Myr to the present day), nonthermal escape is the dominant process. We rely on observations and modeling to construct a

nonthermal escape history for Venus. We consider mechanisms that rely on interactions between solar emission (and solar wind) and the atmosphere (no surface process or impact erosion).

Nonthermal escape efficiency depends mainly on the Extreme UV flux (EUV) which decreases with time, unlike luminosity. The emission variation of the Sun could have been the cause of large changes in the escape rate and the atmosphere [*Kasting et al*., 1984; *Zhang et al*., 1993a; *Jakosky et al*., 1994; *Chassefière*, 1996a, 1996b, *Lammer et al*., 2003a, 2003b; *Kasting and Catling*, 2003; *Smith et al*., 2004; *Bauer and Lammer*, 2004; *Lundin and Barabash*, 2004; *Chassefière and Leblanc*, 2004]. The actual EUV solar flux can be approximated with the following law [*Ribas et al*., 2005]:

$$\text{Flux} = \text{Flux}(\text{present average cycle conditions}) \times [\text{Age}(\text{Sun})/\text{Age}]^{1.23\pm0.1\ 231} \quad (1)$$

where Age(Sun) is set to 4.7 Gyr. This implies that roughly 2.8 Gyr ago the Sun's average EUV flux was 3 times greater than its present value, and 4.5 Gyr ago it was 100 times greater. In our model, the past escape flux is calculated for different periods of past solar emissions from the present-day situation, using solar maximum and solar minimum escape fluxes to extrapolate to the past conditions at ancient times. The exact effect of increased EUV flux on escape is presently not completely known, but a factor 2 enhancement from solar minimum to maximum has been proposed [*Brace et al*., 1987; *McComas et al*., 1986] or factors varying from 2 to 10 over a cycle [*Donahue*, 1999]. On the other hand, more recently, *Fedorov et al*. [2011] proposed that escape might not vary much within a solar cycle, based on recent data and old Pioneer Venus Orbiter data.

Different mechanisms are considered as follows:

1. Sputtering corresponds to a mechanism in which ions produced in the planet's corona or ionosphere can reimpact the neutral atmosphere with an energy large enough to lead to the ejection of neutral atmospheric particles [see *Luhmann and Kozyra*, 1991]. Sputtering is not as important an escape mechanism on present Venus as it is on Mars and other small planets. It is, however, a process that removes some oxygen atoms as proposed by *Luhmann and Kozyra* [1991]. This loss rate is estimated to be 5.0×10^{24} s^{-1} at the present day. It is currently unknown how such an escape rate changed in the past, not directly due to increased EUV flux, but more likely due to the expansion of the atmosphere over up to several planetary radii at early times.
2. During dissociative recombination, ions produced in the ionosphere by UV photo-ionization recombine with electrons and form energetic neutrals. On Venus, hot atoms, O*, produced by dissociative recombination do not reach the escape energy for atomic oxygen (9 eV) [*Hodges*, 2000] and are gravitationally bound to the planet and form a corona [*Lammer et al*., 2006]. It is not known how the mechanisms producing O* evolved in the conditions of early Venus, but the resulting escape is here taken to be negligible.
3. With ion pickup escape, ions produced by photo-ionization, electron impacts, and charge exchanges in the exosphere are dragged along by the moving solar magnetic field lines. We follow modeling by *Kulikov et al*. [2006] to calculate the evolution of ion pickup escape. It uses a test particle model involving particle motion in electric and magnetic fields. A range of best estimates for solar wind plasma density and velocity are tested, in particular for the expected young Sun, and are based on a model of the Venusian thermosphere. A diffusive-gravitational equilibrium and thermal balance applied to the heating of the thermosphere by photodissociation, ionization processes, and chemical reactions is part of the model, as well as cooling by the usual CO_2 IR emission. It is consistent with features observed by the Pioneer Venus Orbiter [*Luhmann*, 1993; *Lammer et al*., 2006]. This results in present-day escape rates of around 10^{25} s^{-1} O^+ for average solar conditions. Loss rates at 4 Gyr before present would amount to around 5.0×10^{27} s^{-1}, again, for average solar conditions. Earlier, it could have been much higher, due to the enhanced EUV flux.
4. Finally, plasma clouds have been observed and can be detached by some instability and lost. Plasma escape due to Kelvin-Helmholtz instability at the Venus ionopause can also be modeled. The model used by *Terada et al*. [2002] calculates the ionopause-solar wind interaction kinetically, in 2-D for unmagnetized ionospheric conditions. It uses a hybrid model and a particle-in-cell code. The model produces escape rates of the order of 10^{25} s^{-1}.

These results correspond to other published models like *Jarvinen et al*. [2009] and *Kallio et al*. [2006] and are consistent with higher escape rates than previously proposed (10^{24} s^{-1}) [*Moore et al*., 1991]. Observational constraints also exist with ASPERA measurements, which point to a 10^{24}–10^{25} s^{-1} range for the present-day

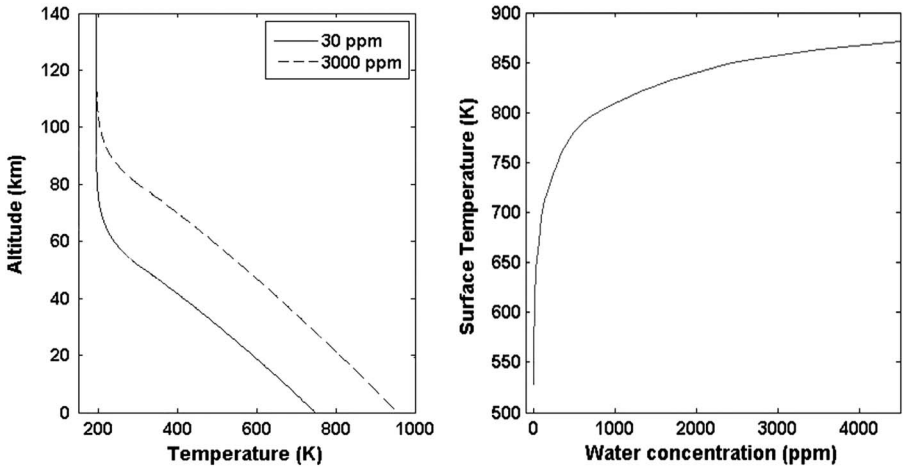

Figure 1. (left) Vertical temperature profiles of the atmosphere of Venus calculated with our radiative-convective gray atmosphere model for two different water concentrations: 30 ppm corresponding to the present-day situation and 3000 ppm to a hypothetical primitive water-rich atmosphere. (right) Surface temperature of Venus as a function of water concentration in the atmosphere.

escape of O^+ at minimum solar conditions. This is consistent with our proposed escape rates. In this study we use a range of different escape efficiencies based on the previously detailed models (Figure 1).

Regarding CO_2, according to our present-day knowledge, its escape flux is likely to be so low as to be impossible to detect with current instruments. We propose a hypothetical maximum value for the present-day escape of CO_2, for test purposes, to be treated as an absolute upper limit. As seen in the results, it does not have a strong influence on our simulations and can be taken as 0 without changing the conclusions or the evolutions detailed here.

2.3. Atmospheric Grey Model

Our model for the atmosphere of Venus and its surface temperature is a modified version of that of *Phillips et al*. [2001]. It is a simple one-dimensional, vertical, radiative-convective atmospheric model. Our model assumes that thermal radiative transfer is grey, so thermal opacity is represented by a single value independent of wavelength. We assume that the atmosphere to be in hydrostatic equilibrium and that the regime is similar to the present day. The greenhouse gases are CO_2 and H_2O, and we consider their ratio to be constant with altitude over the range studied here. This neglects the cold trap effect. It is known that cold trapping is limited in Venus' present-day regime, as water concentration only drops by a factor ~10 between the surface and the top of the clouds.

According to the black body law, we find the following expression relating received and emitted energy fluxes:

$$S = \left(4\sigma T_e^4\right)/(1 - A) \tag{2}$$

where S is the solar flux, σ the Stefan Boltzmann constant, A the albedo (assumed to be 0.7 for present-day Venus), and T_e the effective temperature of the planet, that is, the temperature at which Venus would radiate in equilibrium with the Sun. In the case of Venus, this is 232 K at the present day. The effect of clouds is not modeled separately, which means they are assumed to stay at the present-day state rather than evolving. It is not well known how the clouds on Venus would evolve with changes in atmospheric composition and, in particular, in water abundance. Their composition, albedo, and altitude could change, and it is possible that they could disappear, thus completely changing the atmospheric regime and the surface temperature. Some studies that try to model cloud behavior do exist [*Bullock and Grinspoon*, 2001], but they are more complicated and specialized than our present work and go beyond the scope of this first study. As such, the effect of clouds in visible light is instead taken to be similar to the present day situation and is taken into account by the value of T_e.

S is considered to have varied over time according to the faint young Sun hypothesis. During the last 4.7 Gyr, the solar luminosity has risen from about 70% of its present value to what we observe now [*Gough*, 1981;

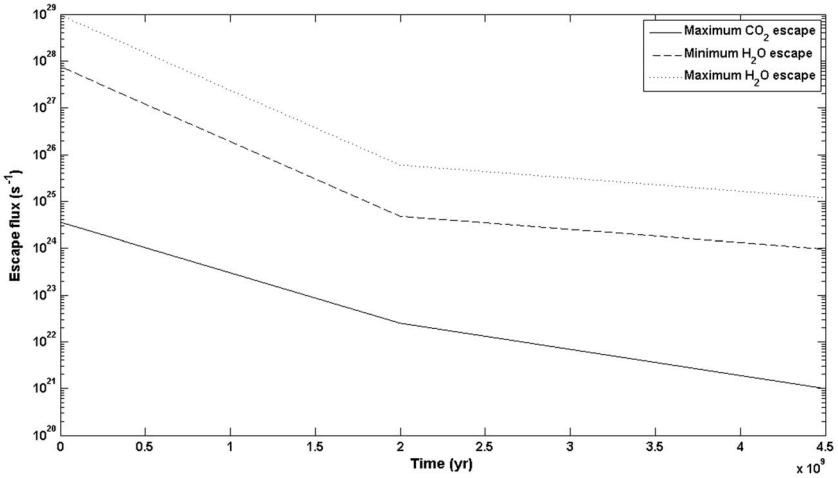

Figure 2. Examples of late total nonthermal atmospheric escape rate evolutions with time, taking into account the different mechanisms described. A range of values is given for water escape, corresponding to the most realistic simulations and observational data from ASPERA. The solid line given for CO_2 is indicative of a hypothetical absolute maximum escape rate used for testing the possible influence of CO_2 losses in the model. Actual present-day CO_2 escape is thought to be so low it cannot be detected with the usual instruments.

Ribas et al., 2010]. We consider a linear evolution for S between these two values, which translates into variations of T_e.

The radiative temperature profile in the atmosphere is given by

$$T_r(z) = T_e \times (\tau(z) + 1/2)^{1/4} \tag{3}$$

where τ(z) is the total infrared opacity depending on the altitude z and is given by (under the assumption that P_{CO2} does not vary much, as evidenced in the results section):

$$\tau(z) = H/(k_B T_s) \times (\kappa_{CO2} P_{CO2} + \kappa_{H2O} P_{H2O})\, e^{-(z/H)} \tag{4}$$

with k_B the Boltzmann constant, T_s the temperature of the atmosphere at the surface, κ the infrared absorption coefficient (for CO_2 and H_2O), P the atmospheric partial pressure (for CO_2 and H_2O), and H the scale height, given by

$$H = k_B T/(gM) \tag{5}$$

with g being the acceleration due to gravity (8.87 m s^{-1} on Venus) and M the mean molecular mass.

At the present day, P_{CO2} is 89 bar, water is thought to amount to 30 ppm, and the total pressure is 92 bar. We use the constraint that surface temperature should be 520 K without any water in the atmosphere [*Pollack et al*., 1980] to determine the ratio of CO_2 and H_2O absorption coefficients.

In the convective layer the vertical temperature profile is given by the following expression:

$$T_c(z) = T_s + \Gamma(T)\, z \tag{6}$$

where Γ is the dry adiabatic lapse rate and is temperature and composition dependent. It is given by

$$\Gamma(T) = -g/C_p(T) \tag{7}$$

where C_p depends on the temperature and is a combination of C_{pCO2} (T) and C_{pH2O} (T) proportional to their relative densities [*Kasting*, 1988]. The expressions of C_{pCO2} (T) and C_{pH2O} (T) are polynomial expressions as proposed by *Abe and Matsui* [1988], with T being the temperature of the atmosphere.

The temperature of the atmosphere at the surface is then found by finding the value of T_s for which the two expressions fit at the tropopause, where radiative and convective gradients and temperature all match, and create a realistic vertical profile (Figure 2).

The initial CO_2 pressure has been taken to be between 50 and 100 bar, but values of 88–89 bar are preferred. Initial water contents of between 0 and 1 bar have been tested. It is likely that some water would be present

in the early atmosphere of Venus due to the later phases of accretion [*Raymond et al*., 2006] and by subsequent cometary input. However, a large water content at/after the end of the hydrodynamic escape (300–500 Myr) is unrealistic, as there is probably no means to remove more than a fraction of a terrestrial ocean of water after that time (typically, of the order of 0.1 terrestrial ocean). We do not address the question of whether Venus had liquid water oceans early in its evolution. While our models favor a dry late evolution, the evolution of the planet during the first billion years could still allow for oceans [*Bullock and Grinspoon*, 2003] as water can be liquid at high pressures and high temperatures given the right conditions. Present data do not exclude this possibility.

2.4. Mantle Convection Model

We use a version of the StagYY code [*Tackley*, 2008], which is a development of the earlier Stag3D code [*Tackley*, 1993] and has been used for various modeling studies for Earth [e.g., *Nakagawa and Tackley*, 2005, 2010; *Nakagawa et al*., 2009, 2010] and for Mars [*Keller and Tackley*, 2009; *Golabek et al*., 2011; *Ruedas et al*., 2013a, 2013b]. Specifically, we use the same model setup as *Armann and Tackley* [2012] for Venus, use similar parameters, and apply the same resolution. This section will describe the main features of the model and code; the reader is referred to the previously cited papers for added details.

A compressible anelastic, infinite Prandtl number mantle is assumed. Physical properties like density, thermal expansivity, and thermal conductivity are depth dependent and are calculated as described in *Tackley* [1996, 1998]. Radiogenic heating decays exponentially with time. Spatial variations are not considered. We use Earth-like values for the concentration of heat-producing elements [*Janle et al*., 1992; *Nimmo and McKenzie*, 1997; *Turcotte*, 1995] with a concentration of 5.2×10^{-12} W/kg at the present day and a half-life of 2.43 Gyr. The phase transitions in the olivine system and in the pyroxene-garnet system are included with parameters based on mineral physics data [*Irifune and Ringwood*, 1993; *Ono et al*., 2001], as discussed in *Xie and Tackley* [2004].

The assumed rheology is Newtonian diffusion creep plus plastic yielding. For diffusion creep we assume a temperature and depth-dependent viscosity following

$$\eta(T, d) = \eta_0 \exp((E + Bd)/RT - E/RT_0), \tag{8}$$

where η_0 is the (reference) viscosity at temperature T_0 and zero pressure, T is absolute temperature, d is depth, E is the activation energy, R is the gas constant, and B is given by $B = \rho g V$, with V the activation volume, g the acceleration due to gravity, and ρ the representative density of the considered region. We use a reference viscosity of 10^{20} Pa s. Realistic values for the parameters are chosen based on laboratory experiments for the upper mantle (dry olivine) [*Karato and Wu*, 1993] and best estimates for the lower mantle [*Yamazaki and Karato*, 2001]. Rheology is independent of composition in this study. We refer to *Armann and Tackley*, [2012] for the viscosity profile (their Figure 1) and discussion of its characteristics.

Plastic yielding is included with a ductile yield stress of 100 MPa following the preferred model of *Armann and Tackley* [2012], because it leads to episodic lithospheric overturn that allows Venus to lose its heat without massive magmatism and can generate a surface with the observed age but still with some present-day activity as observed recently [*Smrekar et al*., 2010; *Shaligyn et al*., 2014]. Additionally, it is a case that is likely to display large temporal variations of surface temperature, as it sits between the two end-member scenarios of continuous mobile lid (low yield stress values) and continuous stagnant lid (high values). A narrow range of slightly different values were tested (80–120 MPa) without changes in the results presented in this work. Brittle "yielding" is also included by taking a yield stress that is the minimum of that predicted by Byerlee's law with a friction coefficient of 0.5 and zero cohesion, and the constant yield stress given above, which mimics semibrittle, semiductile processes in the lithosphere [*Kohlstedt et al*., 1995]. Numerically, yielding is implemented by iteratively adjusting (reducing) the effective viscosity in places where the stress is higher than the yield stress, until stress is brought back to the yield stress.

The surface and core-mantle boundaries are free slip and isothermal. The surface temperature is obtained from the atmosphere model. The core-mantle boundary (CMB) temperature is initially set at 4025 K, fitting a superheated core and in line with previous studies [*Nakagawa and Tackley*, 2010; *Armann and Tackley*, 2012]. A core model allows for its cooling over time and is detailed in *Nakagawa and Tackley* [2004]. The initial temperature field is adiabatic with a potential temperature of 1900 K, plus thin boundary layers at top and bottom and random (white noise) perturbations with a peak-to-peak amplitude of 25 K.

We use a 2-D spherical annulus geometry [*Hernlund and Tackley*, 2008] with 512 azimuthal by 64 radial cells. StagYY uses a finite-volume, primitive variable discretization, solves the velocity-pressure solution using a multigrid solver, advects the temperature field using the MPDATA advection technique [*Smolarkiewicz*, 1984], and uses tracer particles (1 million) to track composition and melt [*Tackley and King*, 2003].

2.5. Melting and Degassing

Melting is treated as in other studies using the StagYY code [*Armann and Tackley*, 2012; *Nakagawa and Tackley*, 2004, 2005, 2010; *Nakagawa et al*., 2009, 2010; *Xie and Tackley*, 2004]. For each cell, at each time step, temperature is compared to the solidus, and if it exceeds that limit, enough melt is produced to bring the temperature back to the solidus (i.e., considering latent heat absorption). Melting consumes only the basaltic content of the mantle, so removal of melt changes in the composition of the mantle. Initially, the composition is set to 20% basaltic component, appropriate for a pyrolytic bulk composition as is commonly assumed for Earth's mantle [*Xu et al*., 2008]. The solidus temperature increases slightly with basalt depletion.

All melt located above a certain depth is assumed to rise to the surface. This limit (the depth at which the melt is less dense than the mantle around it) is set to 600 km, which is Earth-like [*Reese et al*., 2007]. When calculating degassing, we assume that 10% of the magma is involved in extrusive volcanism and can contribute to degassing, while 90% ends in intrusive volcanism [*Crisp*, 1984; *Bullock and Grinspoon*, 1996; *Reese et al*., 2007]. This value is consistent with Earth-like conditions and acts as a middle ground between end-member estimates of 8–15%; it is a commonly used value. All of the volatiles in erupted lavas are assumed to be degassed. This degassing might be overestimated if one considers the high surface pressure of Venus (at present day at least), which can prevent the release of volatiles from the lavas [*Elkins-Tanton et al*., 2007] by an amount that is difficult to constrain.

In our models, the concentration of volatiles in the melt scales linearly with the fraction of mantle mass that has already been melted, from the initial content to the present-day concentration (see below). In most of the simulations (see Table 2), water concentration decreases with time from 100 ppm to 50 ppm as the mantle is depleted. Some simulations investigate different situations, such as constant volatile concentration or higher initial content.

We choose the reference present-day water content of magma to be 50 ppm water, far below the usual estimates for Earth but in line with the assumed depleted and dry state of Venus [*Grinspoon*, 1993], which has already substantially melted and lost much of its water. *Grinspoon* [1993] based this conclusion on the assumption that the present-day atmospheric abundance has to be in or near equilibrium to sustain present water concentrations. It also fits mantle composition estimates [*Namiki and Solomon*, 1998] indicating 5 ppm water, which translates into roughly 50 ppm in the melt. In comparison, Earth has 1% water in its melt. Higher values have been suggested based on comparison with Earth, but no solid proof exists. We explore a range of present-day concentrations from 10 ppm to 100 ppm and also test higher values. Likewise, present-day CO_2 concentrations for our main simulations vary between 5 ppm and 500 ppm, corresponding to a reduced mantle. Due to uncertainties on the state of Venus' mantle and for the sake of completeness, we also investigated larger CO_2 contents, corresponding to a more oxidized state, ranging from 500 ppm to 0.5% (w.) and decreasing by a factor of 5 during the evolution.

Larger CO_2 concentrations would probably accompany commensurate water concentrations. A large amount of water (up to several thousands of ppm) is unlikely to be present while remaining consistent with present-day conditions. *Elkins-Tanton et al*. [2007] proposed that the initial volatile content, under some conditions, could be around 1000 ppm CO_2, in the case of early Earth and Mars. It is, however, likely [*Raymond et al*., 2006; *O'Brien et al*., 2006] that Venus received less volatiles than Earth and Mars. This is in line with work by *Ahrens* [1981] stating that Venus would contain less CO_2 than Earth in its mantle.

2.6. Parameters

The main parameters we used for our simulations are listed in Table 1. When other parameters become important, they are listed in the text. For the general evolution of Venus we ran 60 models that included plasticity in the mantle rheology and only nonthermal escape for volatile loss; the efficiency of volatile escape and degassing were the main parameters varied in those. A further 10 models were included to investigate larger degassing rates than in our reference simulations; these included increased CO_2 content in the lavas

Table 1. Physical Properties

Property	Symbol	Value (Variation)
Planetary radius	R	6052 km
CMB radius	RCMB	3110 km
Mantle depth	D	2942 km
Gravity	g	8.87 m/s^2
Surface temperature (for uncoupled cases)	T_{surf}	740 K
Initial CMB temperature	T_{CMB_init}	4025 K
Specific heat capacity	C_p	1200 J/kg/K
Latent heat of melting	L	600 kJ/kg
Reference viscosity	η_{ref}	10^{20} Pa s ($\eta_{ref} - 2\eta_{ref}$)
Reference yield stress	Y_s	100 MPa (80–120)
Internal heating: present	$H_{present}$	5.2×10^{-12} W/kg
Internal heating: initial	H_{init}	18.77×10^{-12} W/kg
Half-life	t_{half}	2.43 Ga
Solar irradiance (present day)	S	2613.9 W/m^2
Initial CO_2 pressure	P_{CO2}	88.4 bar (0–95)
Effective temperature	T_{eff}	232 K
Reference oxygen escape rate (nonthermal; present day)	E_{ref}	1.895 10^{24} s^{-1} (0.6 E_{ref}–5 E_{ref})
Energy deposition efficiency (hydrodynamic escape)	λ	2.4 (1.2–2.4)
Exospheric temperature (hydrodynamic escape)	T_{exo}	750 K (500–1250)
Hydrodynamic escape start (after beginning of accretion)	t_{h0}	10 Ma
Water concentration in the lavas (present day)	$[H_2O]_{l,p}$	50 ppm water (10–100)

(500 ppm to 0.5%(w.)). Higher water degassing was also investigated but not included here as cases greatly diverged from "successful" ones or required unrealistic escape rates. We ran 10 models that additionally included hydrodynamic escape. A further 10 models tested variation in mantle rheology (with different yield stresses or viscosity); the results of these simulations are in line with those described in the next section, with only some variation in the timing and intensity of the events. For comparison, five models were run with a constant surface temperature (i.e., uncoupled to the atmosphere); the results of those are similar to the models in *Armann and Tackley* [2012].

3. Results

3.1. Differences Between Coupled and Uncoupled Cases

Figure 3 shows distributions of the mantle temperature and composition for the reference case (with plastic yielding and full coupling) at several times during the evolution. The general behavior of the mantle during its evolution is very similar to that described by *Armann and Tackley* [2012]. Progressive melting leads to the generation of basaltic crust on top of the mantle, which during subduction events subsequently sinks to the core-mantle boundary, where it accumulates. An example of the slab-like downwellings involved in this process can be seen in Figure 3 at 1.5 Gyr. Cold lithospheric material is involved. These events are directly related to the spikes of activity seen in the volcanic production rate history and also lead to cooling of the mantle. They appear periodically and are localized, each time occurring in a different specific area. This characteristic makes them a good mechanism to resurface patches of Venus, one after another. They are also are quite fast, lasting between 50 and 100 Myr. A typical evolution of the model over 4.5 Gyr contains around 20 such events.

In addition to these single localized downwelling events, we also observe global-scale mantle overturn events. Such an event is detailed in Figure 4. These events are similar to those described in *Armann and Tackley* [2012]. They last longer—around 100–150 Myr—and involve the whole lithosphere, initiating in one place then propagating around the planet. In the present cases including atmospheric evolution and coupling, however, only one or two of those events are observed, instead of the five to eight found in models without the inclusion of the atmosphere. We also observe propagation from a single initial downwelling to a global-scale overturn, although we do not see an obvious mixing of the mantle as a result of the event. This implies a possible stabilization of the lithosphere (and hence the climate) against large episodic overturn events by the atmospheric feedback.

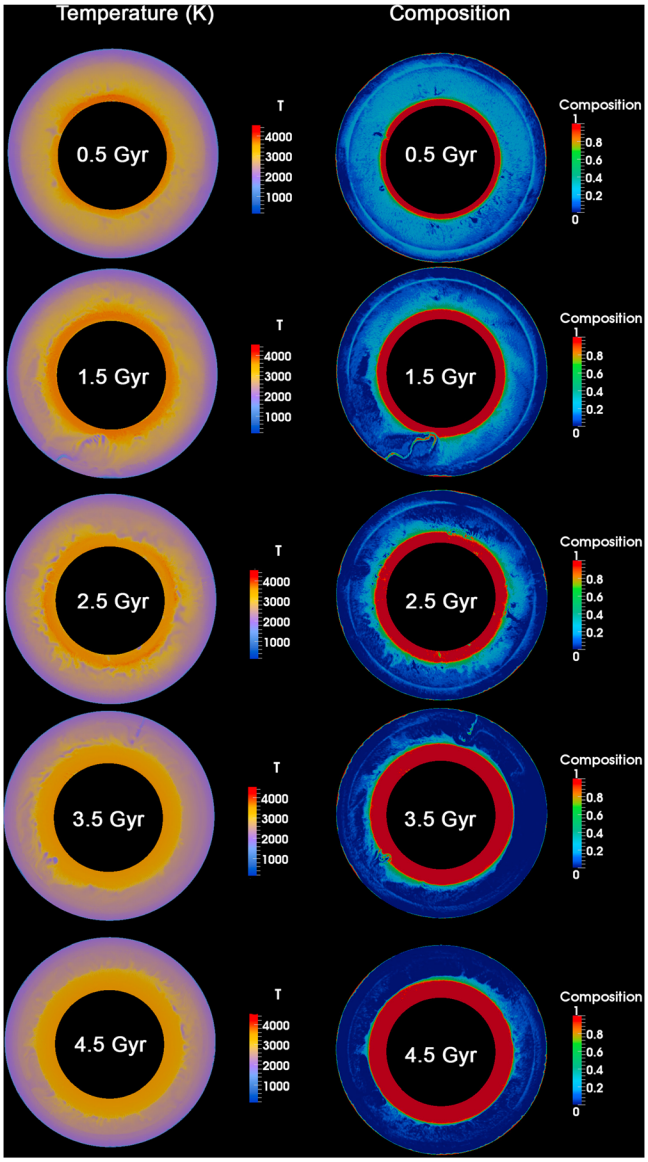

Figure 3. Time evolution of temperature and composition in the mantle of Venus using our coupled model (including yield stress). Parameters correspond to the reference case (see Table 1). Composition ranges from 0 (harzburgite) to 1 (basalt).

Atmospheric coupling modifies some aspects of the mantle evolution of Venus, as compared to constant surface temperature models. While the general aspects of the convection remain similar in both cases with some global-scale resurfacing events (and similar cumulative melt generation and emplacement, or mean volcanic production rates), changes in surface temperature introduce differences in the evolution of the planet.

Venus-like volcanic production (crustal production) rates and mean crustal thickness stay in the same range of values and fit present-day estimates, for the parameters we used here.

Figure 5 shows an example evolution of a constant surface temperature model (uncoupled case, $T_s = 740$ K) for comparison with the results of the coupled reference model in Figure 6. The uncoupled model shows an almost regular sequence of high volcanic activity spikes and longer quiet periods. The overall intensity of volcanism decreases over time and the quiescent eras become longer, but the intervals between volcanic events are quite regular. In contrast, the coupled model does not display this clear periodicity. An obvious succession of volcanic maxima and "downtimes" are still visible, but they are not evenly spaced. The evolution thus looks more chaotic. A clear-cut monotonous decrease in volcanic activity intensity with time is also not always found.

3.2. Volcanism

A summary of the main characteristic features of the evolution of the coupled model for Venus is shown in Figure 6. This case will hereafter be referred to as the reference case. Time evolutions of surface temperature, volcanic activity, and atmospheric content (for the main species H_2O and CO_2) are shown, as well as conductive heat flux at the top and bottom of the mantle and r.m.s. velocity. This simulation includes nonthermal escape and mantle coupling with surface temperature evolution, but thermal escape is excluded. It starts at the end of the possible magma ocean phase, corresponding to a time period starting roughly 70–100 Myr after the end of the accretion.

We first characterize the volcanic history of Venus, as indicated by the time evolution of volcanic production rate. Four main phases are apparent: 0–750 Myr, 750–1500 Myr, 1500–2200 Myr, and 2200–4500 Myr. The exact timing depends on the parameters used, but the phases stay the same.

Early on (typically 50–80 Myr) the first melting occurs, corresponding to the first plumes and downwellings, and the planet enters a high volcanic activity period lasting a few hundred million years. During this time (and

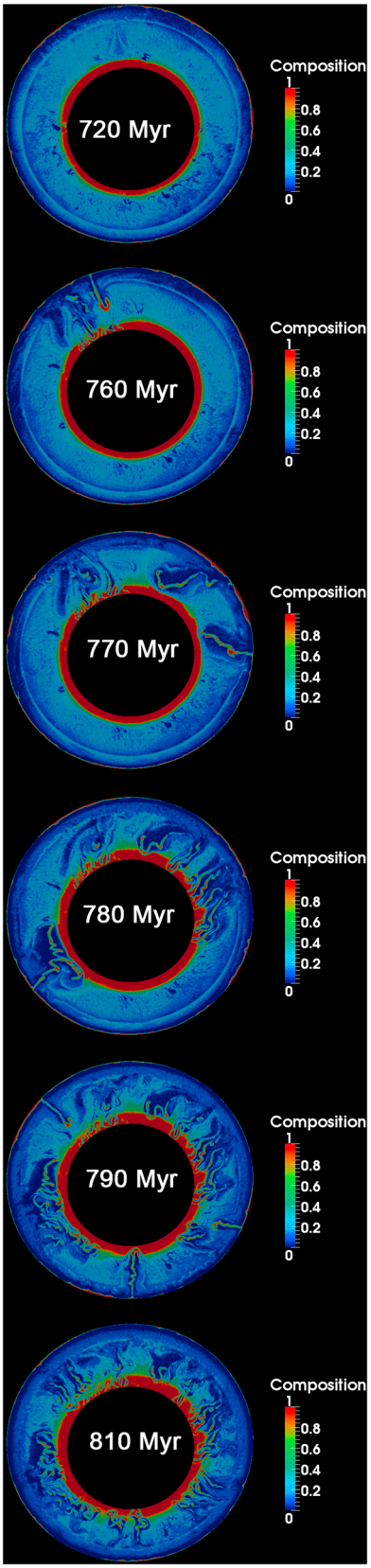

lasting 500 Gyr), volcanism is globally high, with downwellings of cold material occurring one after the other over the whole mantle. The end of this phase is marked by a sharp decrease of volcanic activity as a stagnant lid forms.

After this first period, during the next 750 Myr, volcanic activity remains quite high, although not always at the level of the first period. The background magma production rate is typically 2 km^3/yr, but events producing higher production rates of 4 km^3/yr or more (depending on the simulation) are observed. These are localized events, rather than global-scale ones as observed in the early evolution.

Around 1.5 Gyr, volcanic activity enters a third phase. Magma production rates are lower, with a background rate of around 0.5 km^3/yr, or even lower in some models.

Finally, after 2.2 Gyr, a final phase is observed. Background volcanism stays quite low but more spikes in activity appear, with quiescent periods in between. Maximum magma production rates can be quite high. In this case, a final major magmatic event occurred less than 300 Myr ago. Around 3.10^7 km^3 of magma was produced and placed on the surface, corresponding to a 100 m deep layer over 60% of the surface of Venus. Since 500 Ma ago, the magma production rate averaged 0.5–3 km^3/yr. Those results are in good agreement with rates published by earlier studies from analysis of the cratering rate [*Bullock et al.*, 1993a, 1993b; *Schaber et al.*, 1992; *Strom et al.*, 1994].

Such a recent volcanic rate is consistent with the pristine state of volcanoes observed at the surface of Venus and reports of volcanoes less than 250,000 years old [*Smrekar et al.*, 2010]. It also fits the presence of water and SO_2 in the atmosphere, volatiles that would otherwise be depleted. Numerical values are in line with the lower estimates by *Fegley and Prinn* [1989] or *Bullock and Grinspoon* [2001] but remain too low compared to their upper range (up to 11 km^3/yr for the former and 9.2 km^3/yr for the latter). Volcanic production rates since the last major event are in line with past estimates [*Volkov and Frenkel*, 1993; *Matsui and Tajika*, 1995; *Bullock et al.*, 1993a, 1993b; *Strom et al.*, 1994; *Price and Suppe*, 1994]. For comparison, a list of the main simulations is shown on Table 2. Models including plastic yielding models satisfy realistic evolution parameters (melt production and crust thickness) in the same way as described in *Armann and Tackley* [2012].

3.3. Evolution of the Atmosphere

Through degassing, volcanism has a strong influence on the atmosphere of a planet. We assume that a CO_2 atmosphere is already in place at the beginning of our simulation. Water can be present in the atmosphere at that time or it may have been lost to space early on [*Gillmann et al.*, 2009]. Here we assume that a

Figure 4. Composition field in the reference case, with detail of a resurfacing event. Parameters are also the same as in Table 1. The time of each graphic is indicated on the figure.

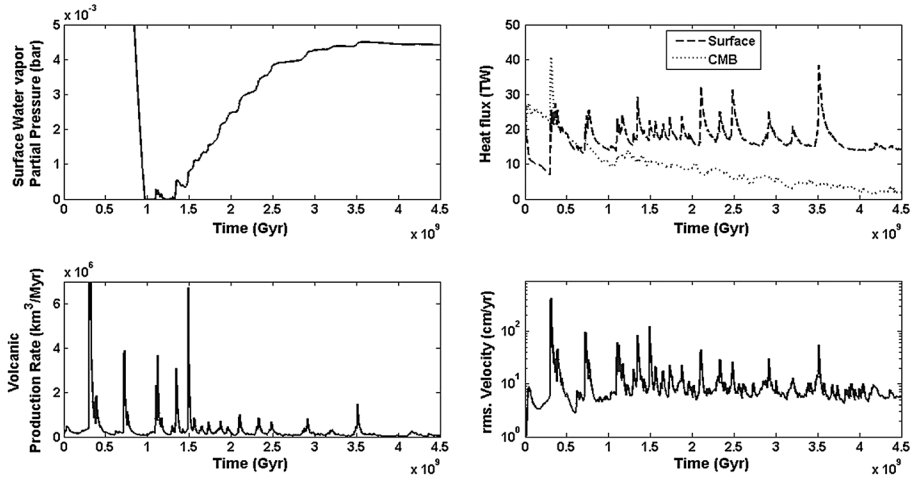

Figure 5. Evolution of Venus for an uncoupled reference case (constant surface temperature, 740 K) to be compared with the coupled reference case shown in Figure 6. We show surface water vapor partial pressure, conductive heat flux (surface and CMB), volcanic production rate, and r.m.s. velocity. Surface temperature is 740 K, although higher water content of the atmosphere would produce higher corresponding temperature, when compared to Figure 6. CO_2 pressure is not shown as its evolution is similar to the coupled case.

small amount of water (0.1 bar) remains in the atmosphere at that time. This accounts for the higher surface temperatures exhibited by the model during the first 1000 Myr.

Indeed, we observe that the surface temperature drops from 950 K to around 540 K, at which it stays for roughly 500 Myr. Small abrupt spikes in temperature (rising to around 600 K then dropping again) can be seen during this period. After this period, surface temperature rises steadily toward around 740 K, at which it becomes somewhat stable. We observe that this behavior is clearly correlated with the water content of the atmosphere.

Early in the evolution of Venus (for the first 1.5 Gyr) solar extreme UV flux is usually high and the amount of energy brought to the atmosphere is high enough to enable a large escape flux. Thus, water is quickly removed and cannot accumulate. Later on (the last 3 Gyr), the energy input is only enough to power the escape of a smaller fraction of the water from the atmosphere. As a result, water can accumulate in the atmosphere, leading to increased surface temperatures.

In contrast to water evolution, for our preferred cases, although CO_2 pressure increases steadily over the 4.5 Gyr evolution of the model there is no noticeable influence of its variation on surface temperature. This is

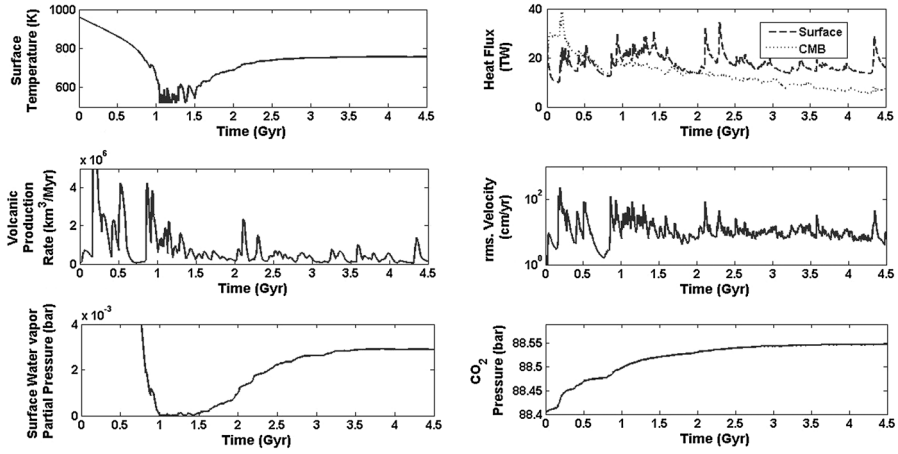

Figure 6. Example of results of the coupled model (hydrodynamic escape not included) at "reference" parameters (see Table 1). We show the evolution of surface temperature, volcanic production rate, surface water vapor partial pressure, and CO_2 partial pressure, r.m.s. velocity, and conductive heat flux at the surface (dotted line) and CMB (solid line).

Journal of Geophysical Research: Planets

10.1002/2013JE004505

Table 2. Summary of the Main Simulations[a]

Case	E/E_{ref}	P_{H20i}^{init} (bar)	$[H_2O]_{i\ p}$ (ppm)	η_{Ref} (Pa s)	Plasticity/Yield Stress (MPa)	Hydrodynamic Parameters λ ; T_{exo} (K)	T_{min}; T_{max}; T_p (K)	t_1 ; t_2 ; t_3 (Myr)	t_{volc} (Ma)
Ref	*1*	*0.3*	*100; 50*	*10^{20}*	*100*	*no*	*522; 954; 745*	*843; 1407; 1937*	*370*
Ref uncoupled	1	0.3	100; 50	10^{20}	100	no	522; 954; 792	1024; Ep. Lid	202
Ref 2 (viscosities)	*1*	*0.3*	*100; 50*	*2.10^{20}*	*100*	*no*	*522; 954; 720*	*731; 1352; 1822*	*505*
Ref 3	*1*	*0*	*100; 50*	*10^{20}*	*100*	*no*	*522; 752; 739*	*20; 1631; 2270*	*290*
Ref 4	1	0.5	100; 50	10^{20}	100	no	772; 970; 789	1540; Ep. Lid	120
Ref 5	1	0.3	50; 50	10^{20}	100	no	522; 954; 701	695; 1609; 2089	429
Ref 6	1	0.3	100; 100	10^{20}	100	no	531; 954; 783	1017; 1421; 1892	553
Ref 7	1	0.3	200; 100	10^{20}	100	no	601; 954; 811	1300; 1454; 2012	451
Ref 8	*1*	*0.3*	*100; 50*	*10^{20}*	*80*	*no*	*522; 954; 732*	*755; 1573; 2083*	*501*
Ref 9	*1*	*0.3*	*100; 50*	*10^{20}*	*120*	*no*	*522; 954; 767*	*883; 1376; 1947*	*536*
Ref no plasticity	1	0.3	100; 50	10^{20}	no	no	522; 954; 769	634; 1008; no S.L.	cont.
Ref Hydro 1	*1*	*0.3*	*100; 50*	*10^{20}*	*100*	*2.4; 750*	*522; 954; 732*	*40; 1670; 2509*	*473*
1	0.6	0.3	100; 50	10^{20}	100	no	894; 954; 903	996; Ep. Lid	619
1 uncoupled	0.6	0.3	100; 50	10^{20}	100	no	890; 954; 905	1083; Ep. Lid	139
1.1	0.6	0.3	100; 100	10^{20}	100	no	899; 954; 912	1007; Ep. Lid	221
1.2	0.6	0.5	50; 50	10^{20}	100	no	927; 970; 927	979; Ep. Lid	481
2	0.84	0.3	100; 50	10^{20}	100	no	861; 954; 873	1167; Ep. Lid	32
2 uncoupled	0.84	0.3	100; 50	10^{20}	100	no	865; 954; 881	981; Ep. Lid	410
2 no plasticity	0.84	0.3	100; 50	10^{20}	no	no	860; 954; 881	1075; 1281; No S.L.	Cont.
2 viscosities	0.84	0.3	100; 50	2.10^{20}	100	no	859; 954; 870	1011; Ep. Lid	399
3	0.96	0.3	100; 50	10^{20}	100	no	765; 954; 800	775; Ep. Lid	501
3 uncoupled	0.96	0.3	100; 50	10^{20}	100	no	781; 954; 822	838; Ep. Lid	451
3 no plasticity	0.96	0.3	100; 50	10^{20}	no	no	755; 954; 817	729; 897 ; No S.L.	Cont.
3 viscosities	0.96	0.3	100; 50	2.10^{20}	100	no	749; 954; 779	754; Ep. Lid	210
4	*0.98*	*0.3*	*100; 50*	*10^{20}*	*100*	*no*	*572; 954; 767*	*1006; 1298; 1644*	*81*
4.1	*0.98*	*0.3*	*100; 25*	*10^{20}*	*100*	*no*	*542; 954; 729*	*961; 1302; 1670*	*371*
4.2	0.98	0.3	100; 100	10^{20}	100	no	591; 954; 779	1098; 1259; 1688	199
5	*1.05*	*0.3*	*100; 50*	*10^{20}*	*100*	*no*	*522; 954; 728*	*904; 1329; 1812*	*476*
5.1	*1.05*	*0*	*100; 50*	*10^{20}*	*100*	*no*	*522; 735; 729*	*20; 1239; 1739*	*217*
6	1.1	0.3	100; 50	10^{20}	100	no	522; 954; 706	810; 1723; 2598	953
6 uncoupled	*1.1*	*0.3*	*100; 50*	*10^{20}*	*100*	*no*	*522; 954; 755*	*1002; Ep. Lid*	*329*
6 no plasticity	1.1	0.3	100; 50	10^{20}	no	no	522; 954; 729	799; 965; no S. L.	Cont.
6 viscosity	1.1	0.3	100; 50	2.10^{20}	100	no	522; 954; 679	801; 1559; 2501	776
6.1	1.1	0	100; 50	10^{20}	100	no	522; 709; 693	22; 1755; 2429	622
6.2	1.1	0.3	100; 100	10^{20}	100	no	522; 733; 785	942; 1639; 2272	228
7	1.6	0.3	100; 50	10^{20}	100	no	522; 954; 599	520; 1220; 1692	710

Table 2. (continued)

Case	E/E_{ref}	$P_{H2O}{}^{init}$ (bar)	$[H_2O]_{i\ p}$ (ppm)	η_{Ref} (Pa s)	Plasticity/Yield Stress (MPa)	Hydrodynamic Parameters λ ; T_{exo} (K)	T_{min}; T_{max}; T_p (K)	t_1 ; t_2 ; t_3 (Myr)	t_{volc} (Ma)
7.1	1.6	0.5	100; 50	10^{20}	100	no	549; 970; 671	878; 1656; 2081	212
7.1	1.6	0	50; 50	10^{20}	100	no	522; 954; 570	499; 1298; 1676	389
8	2.1	0.3	100; 50	10^{20}	100	no	522; 954; 551	150; episodic P.T.	155
8 uncoupled	2.1	0.3	100; 50	10^{20}	100	no	522; 954; 589	827; Ep. Lid	74
8.1	2.1	0.3	100; 100	10^{20}	100	no	522; 954; 606	161; 2117; 2522	271
8.2	2.1	0	100; 50	10^{20}	100	no	522; 640; 559	22; episodic P.T.	270
9	4.2	0.3	100; 50	10^{20}	100	no	522; 954; 522	65; episodic P.T.	624
9.1	4.2	0	100; 50	10^{20}	100	no	522; 591; 522	20; episodic P.T.	339
9.2	4.2	0.5	100; 50	10^{20}	100	no	522; 970; 522	165; episodic P.T.	498
10	5	0.3	100; 50	10^{20}	100	no	522; 954; 522	54; episodic P.T.	549
Hydro 1	1	20	100; 100	10^{20}	100	2.4; 750	522; 1180; 848	51; 1563; 2515	140
Hydro 2	*1*	*20*	*100; 50*	10^{20}	*100*	*2.4; 1250*	*522; 1180; 731*	*45; 1498; 2620*	522
Hydro 3	*1*	*20*	*100; 50*	10^{20}	*100*	*1.2; 750*	*522; 1180; 754*	*70; 1523; 2488*	*361*
Hydro 4	*1*	*20*	*100; 50*	10^{20}	*100*	*1.2; 500*	*522; 1180; 743*	*73; 1559; 2571*	338

[a]Using the base initial CO_2 concentration in the atmosphere set at 84.4 bar. Models with different initial concentrations are less realistic and therefore not displayed here. They follow the same patterns, however. For each simulation, we show its name, the main parameters we used (Efficiency of water escape E/E_{ref}, initial water pressure $P_{H2O}{}^{i}$, initial and present water concentration in the lava $[H_2O]_{i;p}$, reference viscosity η_{Ref}, plasticity/yield stress, and the hydrodynamic parameters (λ; T_{exo})). We also display result values for minimum, maximum, and present-day temperatures during the time evolution of the atmosphere, and the timing of the end of the different phases the mantle goes through over the history of the planet as described in the text. Corresponds to the end of the initial phase is t_1, t_2 to the end of the mobile lid regime, and t_3 to the end of the stagnant lid regime. In some cases, a phase is not present; this has been noted in the table. Finally, t_{volc} corresponds to the time (before present day) of the last major volcanic event in the simulation (resurfacing event). Italicized cases are "successful" ones, relative to present conditions.

due to the very low relative variation of the bulk of the atmosphere (less than 2% during the whole evolution, and less than 0.2% in this reference case), with the majority of the changes occurring early on, during the initial stages of high volcanic activity. CO_2 already provides the bulk of the greenhouse effect in the atmosphere of Venus and without any water would generate surface temperatures above 500 K. Small variations do not significantly alter this effect, meaning that water pressure and its large relative variations are responsible for most of the temperature changes in the model.

In these cases, we used the maximum estimate for CO_2 escape rates. It would not be realistic to expect nonthermal escape to have more than a marginal effect on the evolution of CO_2 pressure. On the other hand, we considered an admittedly small amount of volatiles to be present in the magmas (averaging at around 500 ppm water; *Gislason et al.* [2002], for Earth). Given our assumptions, the degassing rate is low and cannot account for a large variation in CO_2 pressure, neither at present nor in the past. In this respect we agree with the conclusions of *Morschhauser et al.* [2009], finding that even including the outgassing caused by so-called resurfacing events, it is unlikely that Venus' atmosphere has been created progressively from a small number of large volcanic events as postulated by *Lopez et al.* [1999]. Such a growth would require huge CO_2 concentrations in magmas in order to generate the appropriate degassing. We ran a special set of simulations to test large degassing effects. In these cases, contrary to the previous ones, we assumed a composition going up to 0.5%(w.) CO_2, more consistent with an oxidized mantle, which cannot be excluded. Unlike in the previous results, we observe a moderate buildup of CO_2 in the atmosphere, commensurate with CO_2 concentration in the lava. In the extreme case (0.5%(w.)), 12 bars of CO_2 were released. Escape had no effect on

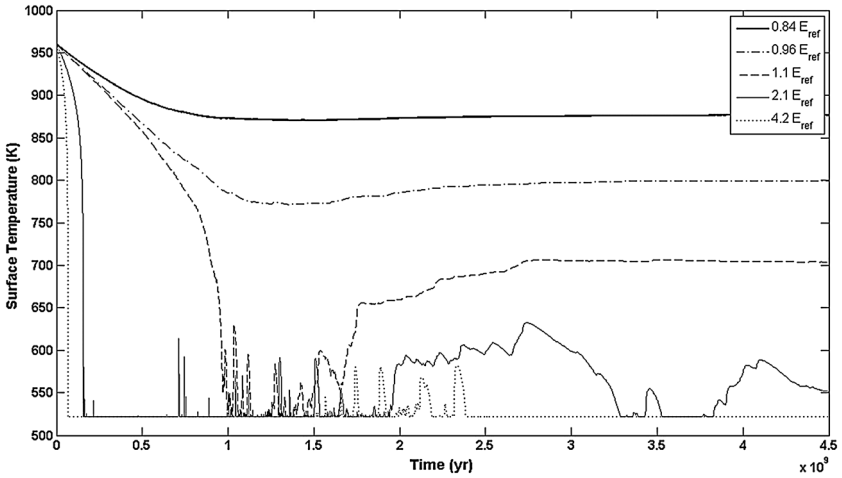

Figure 7. Examples of other surface temperature histories depending on atmospheric escape intensity relative to reference case. All other parameters are set at reference level.

this result. The bulk of the evolution and surface temperature history was, however, unchanged, as the greenhouse effect from CO_2 increased steadily but only slowly over the course of the evolution.

3.4. Influence of Escape Mechanisms

Atmospheric escape is the second mechanism that governs the evolution of the atmosphere. Depending on the escape rate, it is possible to reach a wide variety of present-day surface temperatures. Figure 7 shows surface temperature evolutions for other cases with a varying intensity of atmospheric escape (labeled in comparison with the reference case of Figure 6) and identical initial conditions. A low escape rate (Case 0.84 E_{Ref}) compared to initial water content, leads to present-day surface temperatures that are too high—the final temperature is around 900 K. In this case the bulk of the atmosphere is unchanged, and the evolution is primarily governed by the initial amount of water in the atmosphere.

It is also required that atmospheric escape is not too rapid. In cases 4.2 E_{Ref} and 2.1 E_{Ref} of Figure 7, atmospheric escape dominates the evolution, removing the initial water in less than 100 Myr and then keeping the surface temperature low by efficiently and rapidly removing water that is degassed by volcanism. This leads to low surface temperatures (around 550 K to 600 K) with some short periods of higher temperature corresponding to major volcanic events.

The range of escape rates leading to realistic surface temperatures (700–800 K) is quite narrow—between 0.96 E_{Ref} and 1.1 E_{Ref}. The 1.1 E_{Ref} corresponds roughly to the limit at which all the initial water content can be removed in under 2 Gyr. This seems to be required to reach a realistic range of present-day surface temperatures, thus providing a link between escape efficiency and maximum initial water content in "realistic" cases.

About 90% of the models using this range of escape rates (but other parameters for mantle convection, excluding widely differing cases like stagnant lid simulations which can produce the right surface temperatures but not the right volcanic production rate) converge toward realistic present-day temperatures. High volcanic degassing can moderately change this limit (due to the grey atmosphere model) and requires higher escape rates for water. A higher CO_2 degassing rate has a minor impact on the global evolution apart from leading to a moderate build up of the CO_2 atmosphere. A lower volcanic degassing rate stretches the range of values commonly used for water and CO_2 concentration in the mantle and is thus unlikely. Only massive volcanic fluxes lead out of the realistic present-day temperature zone (more than several times the maximum water concentration from Table 1). Degassing nevertheless has a strong influence on the exact evolution of surface temperature.

3.5. Integrating Hydrodynamic Escape

To complete the atmospheric model we added the effects of hydrodynamic escape to the nonthermal processes considered in the previous section. We adapted primordial conditions (increased initial water

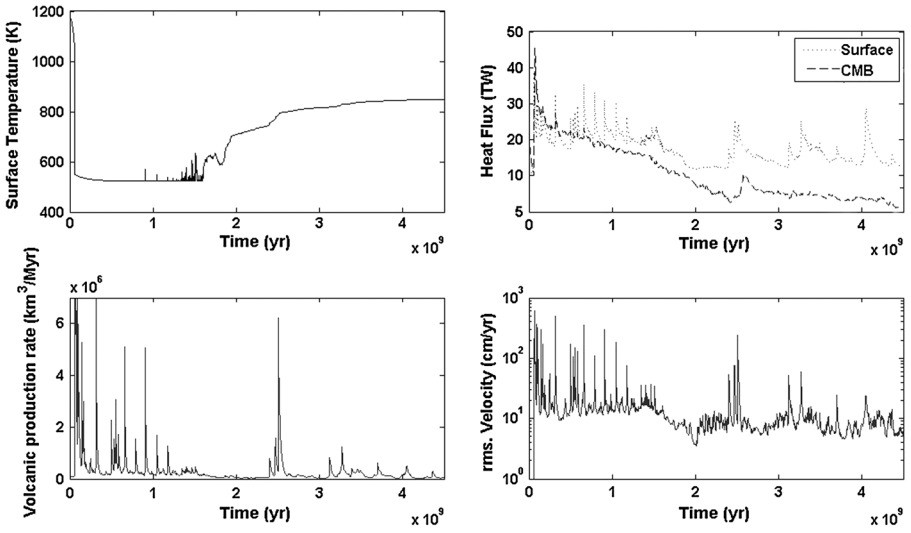

Figure 8. Evolution of the coupled model including hydrodynamic escape simulation. We show surface temperature, surface and CMB heat fluxes, volcanic production rate, and r.m.s. velocity. Initial water content is increased to 20 bar partial pressure. Water concentration in the lava is fixed at 100 ppm. Other parameters are the same as reference case.

content up to 20 bars) to take into account this new escape flux. Figure 8 shows an example of the evolution of surface temperature, magmatic production rate, heat flux (at the surface and core mantle boundary) and r.m.s. velocity. The evolution follows the same pattern described above for cases with no hydrodynamic escape but with a more marked behavior. The initial surface temperature is higher (around 1200 K), which is reasonable when the possibility of an early magma ocean is considered. This is explained by the high water pressure early on. Indeed, just after the magma ocean has frozen (after 50–100 Myr), it is still possible to deliver large amounts of water to Venus (see a self-consistent Venus history, *Gillmann et al*. [2009]). At the time considered here (before 500 Myr), hydrodynamic escape can still operate if there is water in the atmosphere. The evolution of surface temperature reflects this, as it decreases very fast. After 500 Myr, hydrodynamic escape no longer contributes to the escape rate of water. The late evolution is therefore similar to that in previous models (see Figure 6). Volatile contents evolve in the same way as in the reference case.

Although the scenarios including hydrodynamic escape are likely to be more "realistic," we choose to use the reference model without hydrodynamic escape as an illustration of feedbacks between the atmosphere and mantle convection, as it allows a clearer view of the mechanisms involved.

3.6. Evidence for Different Periods and Regimes

Figure 9 documents changes in the behavior of the mantle that depend on the range of surface temperatures at a given time. Viscosity, temperature, composition, and horizontal velocity are shown as function of mantle depth. Figures 9a–9d correspond to different times, respectively, the early volcanic maximum (an overturn event), the low surface temperature era (at 600 Myr, $T \sim 550$ K), when the temperature has just risen ($T \sim 700$ K, around 2 Gyr), and after the second volcanic maximum (around 3.5 Gyr). Viscosity, composition and temperature do not exhibit large variations between the different cases shown. The evolution of viscosity can show a low viscosity zone near the bottom of the mantle during later evolution, corresponding to a moderate increase in temperature in the region of pooled subducted crust.

Horizontal velocity varies most between cases. During an overturn event, it reaches high values all over the mantle, with particularly large velocities near the surface and top of the mantle. This is expected for a large event involving the whole mantle. This period of large velocities is short (a few tens of millions of years).

During the low temperature period (Figure 9b) following the massive volcanic maximum, horizontal velocities remain large (typically a few cm/yr), corresponding to a moderate to high volcanic activity and a mobile lid (facilitated by plastic yielding of the lithosphere). The lid is active most of the time with only a few brief quiescent periods.

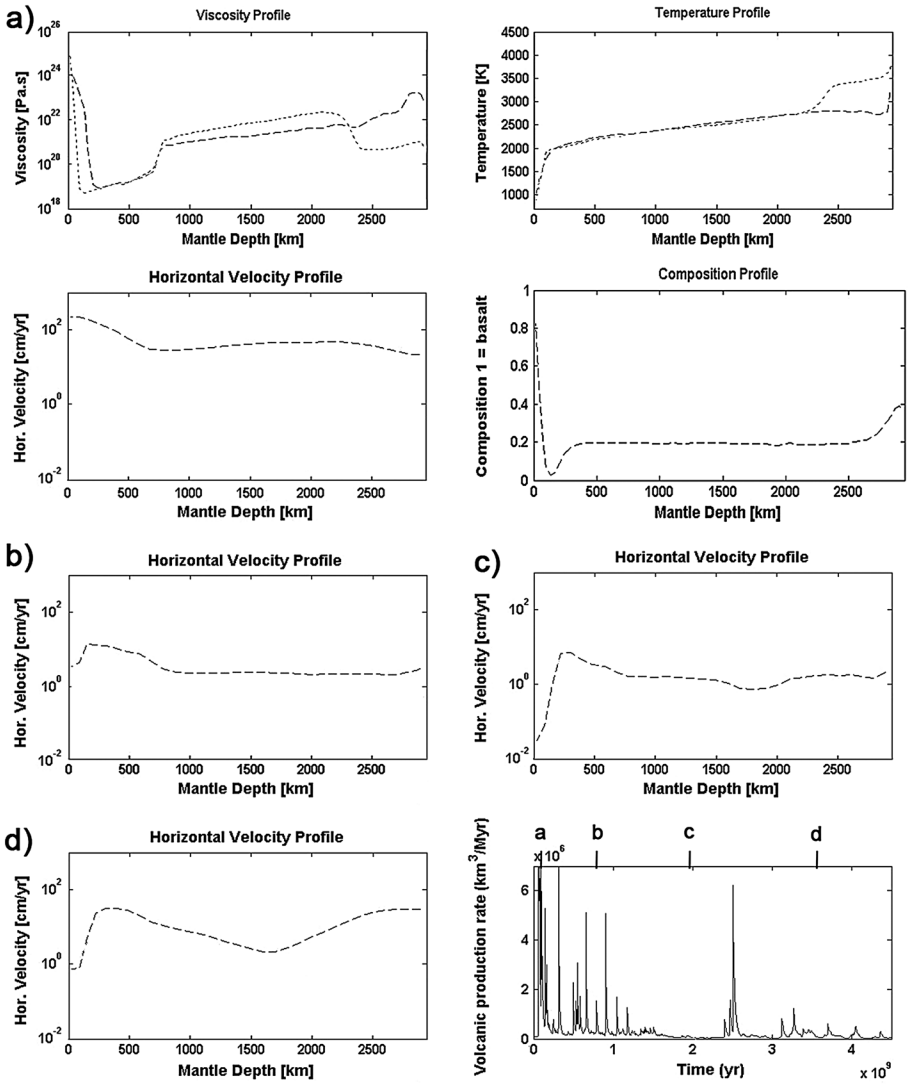

Figure 9. Coupled model including hydrodynamic escape. We show the horizontal velocity profiles at four different times. Other profiles are included for the first time (viscosity, temperature, and composition) but are not repeated for the others, as they do not change significantly. The dotted lines correspond to final (present-day) state of the model. (a) During early activity when plumes reach the surface (100 Myr). (b) During mobile lid phase (800 Myr). (c) During stagnant lid phase (2 Gyr). (d) During episodic lid phase (3.5 Gyr).

When surface temperature increases (Figure 9c) and volcanic activity declines, horizontal velocities decrease sharply, particularly near the surface. The upper regions show horizontal velocities ranging between 0.01 and 0.1 cm/yr. This suggests a sluggish evolution and a more stagnant lid compared to the previous stage.

Finally, the last era (Figure 9d) has moderately low near-surface velocities (less than 1 cm/yr here but reaching values of the order of 1 cm/yr in some cases) compared to previous eras but still shows higher values in the upper mantle, which is due to small-scale convection. This situation is not completely stable and short-lived episodic events occur, marked by higher velocities.

Magmatic production rates display the same eras (Figure 10). This underlines the features of the evolution, as lower temperatures seem to be associated with higher magmatic activity than the subsequent higher-temperature era (2 Gyr to the present day). The following observations are consistent with all our models, and another example can be seen in Figure 8. Changes in magmatic activity are correlated with surface temperature. Generally speaking, low temperatures are associated with higher magmatic production rates.

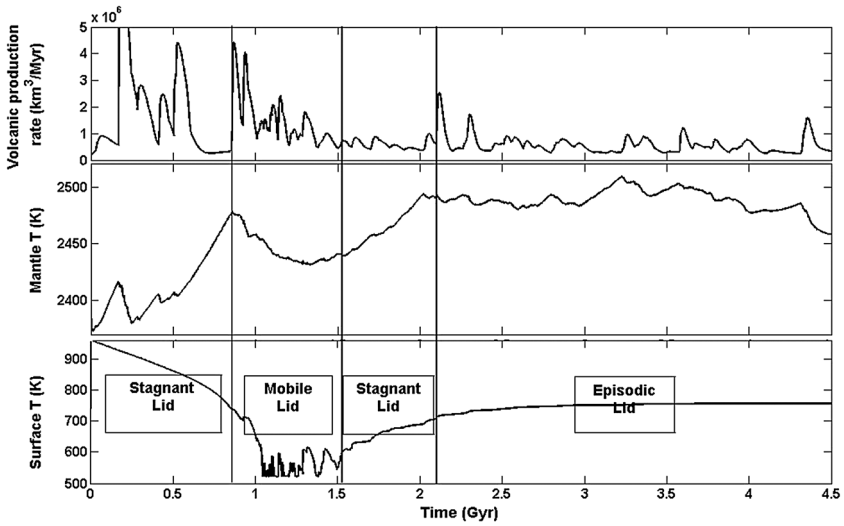

Figure 10. Comparative evolution of volcanic production rate, surface temperature, and volume averaged mantle temperature with time for the reference case. Also indicated are the different convective regimes. The transition from mobile lid to stagnant lid is progressive. Early evolution (before 700 Myr) follows an episodic, but mostly stagnant, lid pattern.

The first transition occurs when surface temperature first drops from above 800 K to around or less that 650 K. If this initial decrease in surface temperature happens very early, it can cause a strong initial volcanic maximum, rather than the extended period of high activity observed in the reference case (Figure 6). As before, in this low–surface temperature era convection exhibits characteristics of the mobile lid regime.

The second transition is more progressive and happens when the surface temperature increases to around 650–750 K due to volcanic degassing. This is particularly clear in Figure 8, where an 80–100 K rise (at 1.5 Gyr) leads to a rather abrupt shutdown of most of the melt production and the creation of a stagnant lid. Such a state does not last long, as surface heat flux drops; hence, the mantle heats up.

Around 2–2.5 Gyr the third transition occurs, marked by a magmatic production spike corresponding to a massive global overturn event, probably resulting from the heating up of the mantle during the previous 500 Myr. This event can also be seen on the heat flux and r.m.s. velocity graphs (Figure 6). This is followed by episodic activity. During the subsequent evolution, heat fluxes are in line with expectations from previous models [*Armann and Tackley*, 2012]. The CMB heat flux at the present day is around or below 10 TW, while values of order 30 TW are observed early on.

From the r.m.s. velocity (Figure 8), two main eras can be identified. The first corresponds to the low–surface temperature era (0–2 Gyr) and is characterized by a high background velocity (~10–20 cm/yr) with frequent and regular spikes with much higher values. When the planet enters the second phase at around 2 Gyr, Vrms drops to lower values. The present-day Vrms is 5 cm/yr. The main difference between these two phases is the regularity of the early phase against the more chaotic behavior of the late evolution.

Our simulations show that magmatic production is increased when the temperature drops below 600–650 K and is reduced when the temperature rises above this limit and stays in the 650–850 range. Higher temperatures (above 900 K) have not been tested extensively and, while unrealistic for recent Venus, have been predicted by some evolution models [*Noack et al*., 2012] to occur a couple of billion years ago. They may have a positive effect on melt generation, but more extensive testing is required to assess their exact effects.

Here we observe transitions from a mobile lid regime (or plate tectonics-like behavior) to a stagnant lid regime and then to an episodic lid regime as the surface temperature first decreases then increases. Such a transition is qualitatively consistent with *Lenardic et al*. [2008], who found that high surface temperatures could shut down an active lid mode of convection. The exact mechanism for this requires further investigation, but generally a lower surface temperature will result in higher viscosity and perhaps higher stress, making it easier to reach the yield stress [*Lenardic et al*., 2008; *Moresi and Solomatov*, 1998; *Trompert*

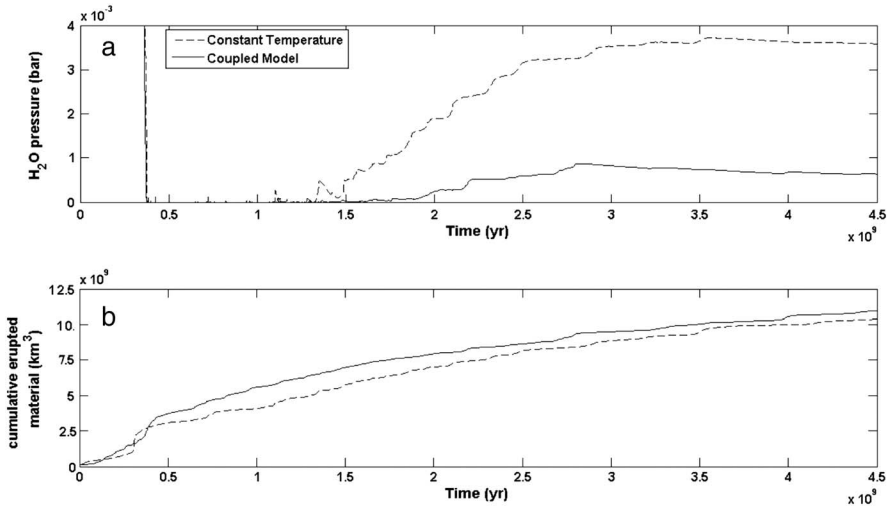

Figure 11. Comparison between coupled and uncoupled (constant surface temperature) models; reference case. (a) Evolution of atmospheric water partial pressure for both cases together with total cumulated eruptive melt production. Parameters are the same as reference except atmospheric escape, set at 1.5 E_{ref}. (b) Profiles for volcanic production rates over time for coupled and uncoupled models.

and Hansen, 1998] and enter a mobile lid regime, in which the mantle is able to ascend to very shallow depth under spreading centers, and hence generate much melt.

In the stagnant lid mode, heat transfer across the lithosphere is inefficient; thus, the mantle heats up. Episodic overturn due to lithospheric yielding appears to be triggered by the mantle reaching a certain temperature rather than by the lid reaching a certain thickness as earlier predicted [*Turcotte et al.*, 1999], because the lid reaches an equilibrium thickness maintained by small-scale convection [*Armann and Tackley*, 2012]. Plumes rising from the core-mantle boundary appear to help initial overturn, because they generate locally thick crust that results in large local stresses.

A consequence of convective regime changes is the modification of atmospheric volatile content. However, the effects of atmospheric coupling can be quite subtle, as exemplified in Figure 11, which shows the evolution of cumulative volcanic production and water content for coupled and uncoupled (constant surface temperature) models with an escape rate of 1.2 E_{ref}. The total amount of magma erupted at the surface is approximately the same for both cases, slightly higher for the coupled model. However, the amount of water in the atmosphere is dramatically different, with the uncoupled model having a much larger present-day accumulation of H_2O. The timing of magmatism is the critical difference: in the coupled model much magma is produced early on, at a time when atmospheric escape is rapid enough to remove water efficiently. In the uncoupled model proportionally more magmatism occurs later, when escape is much slower and water can accumulate in the atmosphere. This phenomenon is amplified by the depletion of the volatiles in the mantle, i.e., the mantle water concentration is decreased by earlier magmatism, so in the late evolution less water is released per km^3 of erupted magma in the coupled model. The combination of these effects efficiently lowers the present-day water concentration in the atmosphere of Venus and thus the present-day surface temperature from around 800 K to 700 K. It also occurs in most of the simulations we ran except those in which the surface temperature was kept above 800 K due to low escape rates (0.96 E_{ref} and below).

4. Discussion

4.1. Late Escape

One of the main parameters varied in our simulations was the non-thermal escape efficiency. The range 0.96–1.1 E_{ref} leads to the most realistic present-day surface temperatures. It is unlikely that the actual escape rate differs strongly from these published estimates [*Luhmann*, 1993; *Lammer et al.*, 2006; *Jarvinen et al.*, 2009; *Kallio et al.*, 2006] at the present-day, although a slightly higher escape rate might be possible, depending on the effect of the solar cycle.

It should be noted that in all the cases displaying a 700–780 K present-day surface temperature that we have so far tested, the atmospheric water concentration reached a near equilibrium toward the present day.

Some cases display large temporal variations during their late evolution, with surface temperature changing by several tens of Kelvin over short timescales, but none of these cases have realistic present-day temperatures. This is due in part to the assumption of a volatile-depleted mantle at the present day. Late degassing is therefore slow, and in order to preserve late water content in the atmosphere, escape rates need to be low.

In our study we did not directly compute the evolution of the D/H ratio over time in every simulation, mainly because we focus on heavier species and their influence on the global evolution. Nonthermal escape rates we use for oxygen, however, are compatible with recent estimates for hydrogen loss rates [*Barabash et al*., 2007] and a stoichiometric relation between H and O (1 O for 2 H). These values lead approximately to the measured present-day enrichment factor of Deuterium on Venus relative to Earth during the last 4 Gyr. A more detailed view will require additional modeling, in particular relative to possible D/H ratios in the mantle, which could be different from the Earth's.

4.2. Degassing

We used a standard value for the water concentration corresponding to a present-day "depleted" mantle. Early values, before any melting occurs, are higher. Such a situation seems realistic when observing the respective surface conditions on these two planets. Indeed, a low water content might also be required to explain the present-day 30 ppm water in the atmosphere of Venus, depending on how long ago the last major volcanic event occurred. It might also be needed to fit the D/H ratio.

Reasonable variations in primitive magma water concentrations (several tens of ppm up to 1000 ppm) do not significantly affect the outcome of the model, particularly when hydrodynamic escape is taken into account, as most of the surplus water is lost to space. However, obtaining the actual present-day situation requires a fine balance between late escape and degassing. The relatively low water concentration values used here (10–100 ppm in the melt) usually lead to the best cases.

Some studies (for example, *Lopez et al*. [1999]) used larger volatile contents in Venus' mantle, using Earth as a reference. Values can range from 200 ppm to 5000 ppm or more for CO_2 and can be even larger for water. In this case, the simulations we tested show that a moderate buildup of the CO_2 in the atmosphere can occur, but it does not significantly modify the rest of the evolution of the planet. Note that we are limited to evolutions excluding very large variations of CO_2 pressure (i.e., situations with low CO_2 pressures that are strongly different from present-day Venus) due to the atmospheric model we use. However, most evidence, including isotopic considerations like D/H ratio and ^{40}Ar abundances, still point to a low water concentration. *Kaula* [1999] even suggested that most of the water would have been degassed and lost as early as 100 Myr after the formation of the planet. This would also be consistent with models of planetary accretion, which suggest [*Raymond et al*., 2006; *O'Brien et al*., 2006] that Venus could have been formed with up to 3 times less water than Earth.

This underlines the importance of constraining degassing history and calculating the evolution of ^{40}Ar in the atmosphere. The observed deficiency of ^{40}Ar might be consistent with low volcanism since the last resurfacing event [*Kaula*, 1999]. Further work on this topic will constitute an improvement of our model, as a quantitative study of the ^{40}Ar history will provide a very useful constraint on our simulations in future.

The second uncertainty related to degassing is the degassing efficiency; that is, the ratio of the mass of gases reaching the atmosphere and the mass of volatiles entering the melt. This ratio incorporates, but is not necessarily equal to, the ratio of eruptive to intrusive volcanism. For the sake of simplicity we use a fixed value of 10% in accordance with numerous works [i.e., *Kiefer*, 2003; *Crisp*, 1984; *Greeley and Schneid*, 1991; *Noack et al*., 2012] and as a middle ground between the extremes of 1:5 to 1:12 for the ratio of extrusive to intrusive volumes in Earth. This parameter, however, is poorly constrained, especially in the case of Venus. Some authors have advocated higher-efficiency parameters (for example, *Grott et al*. [2011] chose 40% without detailed explanation, or *Hirschmann and Withers* [2008]). The degassing process is also much more complex than what is taken into account here. In particular, nonvolcanic degassing might be important (see *Burton et al*. [2013], for the Earth). In this case a 10% efficiency would be considered a low value compared to the overall degassing on Earth.

Fortunately, our model can provide a fair approximation of the results that would be obtained with higher-efficiency factors by looking at simulations using higher volatile concentrations (10% efficiency and

1000ppm CO_2 being roughly equivalent to 20% efficiency and 500 ppm CO_2, for example). Only the extreme cases featuring massive degassing (high efficiency and high concentrations) cannot be estimated this way because we did not run simulations for these parameters. It is only in this particular case, with such parameters, that a substantial buildup of the CO_2 atmosphere occurs, which changes the atmospheric conditions too much for us to study it with precision with the present model.

The degassing situation on Venus, however, is clearly different than what we observe on Earth. We must keep in mind that the high surface pressure can strongly reduce the efficiency of degassing, in the same manner as the degassing of rocks is impaired at the bottom of an ocean on Earth, which can lead to very inefficient degassing [*Elkins-Tanton et al*., 2007]. This has not been taken into account in this study because of the many uncertainties it can introduce. Due to this process, it could be that we are actually overestimating the degassing in this work. It is, however, difficult to say by how much.

4.3. Atmosphere

The atmospheric model we use is kept simple and straightforward in order to allow it to be easily applied to different planetary conditions (such as other planets). Despite the inaccuracy of gray radiative models of Venus (lack of minor radiatively active species and no pressure-broadened absorption bands leading to a very simple vertical profile—see Figure 1—compared to the actual Venus situation), it fulfills its purpose of generating coupling between atmospheric processes and mantle dynamics, letting atmospheric greenhouse gases modify the boundary condition for the convection. The general evolution of the surface temperature is obviously affected by the choice of atmospheric model. and it is possible that the response of temperature to degassing could be overestimated. This, however, is mostly the case for small degassing events. It affects mainly the short-term low-intensity events rather than major trends of the evolution like early massive escape or late water vapor replenishment, which are the main topics in this work and the cause of the feedback.

The main limitation of the atmospheric model is that it is based on the present-day situation, but conditions may have been quite different in the past due to changes in solar input and volatile concentration. If Venus' past atmosphere was substantially different from the present-day one, significant errors could be made. For example, cold trapping is not efficient on present-day Venus, but it might have been during Venus' early evolution. Likewise, it is not well known how Venus' clouds are affected by different water concentrations: at the present day their effect on surface temperature is only ~20 K but more water would alter their composition, and thus their albedo and altitude. They might even disappear, in which case the planet's effective temperature (T_e) may approach 290 K, leading to surface temperatures easily exceeding 1000 K. In most of the cases here (i.e., post magma ocean), water concentration stays at low levels comparable to present-day conditions, thus minimizing the issue. The exception is thus limited to the very early history (not modeled here), with its very dense steam atmosphere. In any case, at that time several other aspects were different, such as the possible presence of a magma ocean; to study this era, a new set of models would be required (see *Marcq* [2012] for the atmospheric part and *Elkins-Tanton et al*. [2007] for the magma ocean). It is, however, likely that the atmosphere cooled down early, and the magma ocean froze (on a timescale of around 10 Myr). Our simulations are consistent with this latter hypothesis.

Our present models exclude SO_2. As a short-lived species, it could enhance the greenhouse effect for short periods of time after volcanic events [*Solomon et al*., 1999]. However, on Venus increased SO_2 could lead to lower temperatures due to increased cloudiness [*Bullock and Grinspoon*, 2001]. A future improvement of our model could follow *Bullock and Grinspoon* [2001]. Another possibility is to use the one-dimensional radiative-convective model of the thermal structure of planetary atmospheres developed recently by *Robinson and Catling* [2012], which has yielded results for a variety of planetary bodies, proving its flexibility.

4.4. Additional Escape Mechanisms

Several mechanisms of volatile removal are neglected here. Both crustal alteration and impact erosion have been suggested as additional mechanisms for atmospheric escape. Crustal erosion is likely to depend on volcanic production rates, as the depth of alteration is thought to be small (less than several tens of centimeters) [*Saito et al*. 2007], and diffusion of oxygen in basaltic melts is of the order of 1 mm/d [*Wendlandt*, 1991]. Additionally, the thick atmosphere causes surface pressure to be similar to that of the oceanic floor at 1 km depth on Earth [*Head and Wilson*, 2003]. Under those conditions, it is likely that not all the volatiles are

degassed into the atmosphere, thus also limiting the diffusion of atmospheric volatiles into the magma. Erosion of the surface could speed up the process, but this was estimated to be around 10^{-3} km^3/yr [*Arvidson et al*., 1992], which is quite negligible.

Impact erosion, on the other hand, has been suggested to have a major effect [*Ahrens*, 1993], perhaps capable of blowing off the atmosphere of Venus with a single giant impact (800 km radius at 20 km/s). Such a collision would most likely occur very early in the evolution of the planet, as did the moon-forming impact. The effects of a smaller (100 km radius) impact might still be significant. In recent years, on the other hand, new studies [*De Niem et al*., 2012; *Shuvalov*, 2009] have contradicted this view and found that impact erosion would be a minor effect, one that could be balanced or even exceeded by the input of volatiles the impactor would bring. Such an issue is still unresolved and our future work will include models accounting for such events and their long-term consequences for the evolution of Venus.

4.5. Mantle Convection and Coupling

Our results display a volcanic evolution consistent with common assumptions and studies concerning Venus. We observe (i) very recent volcanism, which is in line with recent observations of the surface of the planet based on visible and thermal spectrometer imaging on Venus Express [*Smrekar et al*., 2010], (ii) catastrophic resurfacing events [*Schaber et al*., 1992 ; *Nimmo and McKenzie*, 1998] caused by lithospheric overturn [*Parmentier and Hess*, 1992; *Turcotte et al*., 1999], (iii) episodic volcanic activity during the last period of the evolution (last 2 Gyr), and (iv) transitions between convective regimes under the influence of evolving surface temperature (plate tectonics-like to stagnant lid to episodic lid).

Such a picture of volcanic activity is consistent with estimates for the age of the surface of Venus (190 Myr to 600 Myr on average) [*Strom et al*., 1994]. Secondly, the localized nature of most of the major processes could be responsible for the large lateral variations in the ages of the terrains on Venus, leaving patches of surface untouched while covering others [*Ivanov and Head*, 1996]. The volcanic production rates we model are enough to resurface a significant part of the surface of Venus during the last 500 Myr, with one event or two at most. The volcanic activity between these events is comparatively low and is consistent with past estimates (0.01–0.15 km^3/yr, according to *Strom et al*., [1993]).

As the age of the surface of Venus prevents us from gaining more insight into its history, many have speculated on possible past events and volcanic activity [*Nimmo and McKenzie*, 1998; *Hauck et al*., 1998; *Reese et al*., 2007; *Turcotte*, 1995]. Here we propose that changes in surface conditions have played a major role in the evolution of the planet and that surface temperatures have directly affected volcanic activity and mantle convection over time. In this, we join *Lenardic et al*. [2008] who found a mechanism by which a surface temperature increase would favor stagnant lid convection. The mechanism is based on the influence of temperature on the strength of lithosphere and the vigor of the convection. Such a behavior and sensitivity to temperature has also been exhibited by models of novae formation on the surface of Venus [*Gerya*, 2014].

We propose that a plate tectonic-like regime may have occurred early in the evolution of Venus, at a time when the surface temperature was lower than at the present-day (500–600 K). However, this regime would have stopped several billion years ago when greenhouse gases accumulated in the atmosphere and raised the surface temperature to around 700–800 K, causing a switch to stagnant lid mode. A stagnant lid would lead to the accumulation of heat in the mantle of Venus (in the same way as suggested by *Nimmo and McKenzie* [1998]). Once a critical situation is reached, a lithospheric overturn and resurfacing event is initiated, perhaps assisted by a plume from the CMB. This was also suggested by *Herrick* [1994]. This critical situation corresponds to a state where the convective stress becomes again comparable to the plastic yield stress. While the mobile lid regime has removed heat from the interior, the following stagnant lid has allowed it to accumulate again, leading, in time (0.5–1 Gyr), to the event.

After this event, an episodic lid regime takes place with quiet periods interspersed by volcanic activity spikes, and marked by sinking downwellings of dense lithospheric material. At that later time, mantle convection is strong enough to break the lid before it thickens, due to the heat that has not yet been evacuated from the mantle. This situation is in line with *Turcotte's* [1993] suggestion of an alternation between stagnant lid like behavior (with a relative thickening of the lithosphere and surface quiescence) and active lid periods. It also ties in with suggestions by *Phillips et al*. [1992] that a realistic approach of present-day Venus would include

localized resurfacing in different places of the planet, rather than just one global event or constant, continuous, low-to-medium intensity, activity. Most of our simulations show this pattern.

In summary, mobile lid behavior is mainly determined by the strength of the lithosphere compared to convective stresses (which are affected by temperature). The main difference between Earth and Venus is likely the presence of liquid water in Earth's surface environment, which reduces lithospheric strength through the formation of weak hydrous minerals, reducing fault friction by pore pressure and fluid overpressure (when fluids are released from hydrous minerals), and so on. While it has previously been hypothesized that Venus' dry mantle prevents the formation of an asthenosphere, and an asthenosphere is important for plate tectonics, we note that (i) viscosity profiles calculating using laboratory rheological parameters do predict an asthenosphere even for dry conditions [*Armann and Tackley*, 2012]—the absence of water increases viscosity equally at all depths, which is easily offset by an increase in mantle temperature; and (ii) numerical simulations show that a mobile lid regime can exist without an asthenosphere [*Tackley*, 2000a], although an asthenosphere leads to a more Earth-like form of plate tectonics by sharpening plate boundaries and making plates more rigid [*Tackley*, 2000b].

Two previous works can be compared directly to our present results.

The first is *Phillips et al*. [2001], who used a similar (albeit simpler) atmospheric model and a parameterized model of mantle behavior. Their results differ from ours in exhibiting a positive feedback of temperature, in which increased surface temperature leads to increased partial melting. Here we obtain the opposite result. Our mechanism results in a stabilization process, while theirs further destabilizes the planetary conditions. This difference is due to their use of a parameterized mantle model that cannot account for changes in convective regime as a fully dynamical model can.

The second study is by *Noack et al*. [2012], hereafter referred to as NBS2012. Their work is based on premises similar to our own, although their modeling assumptions and results differ somewhat. Their basic approach to coupling the atmosphere and mantle convection is similar to our own. They also take into account degassing based on mantle melting, and the principles of melt extraction and volatile release into the atmosphere are the same. Likewise, they consider atmospheric escape as the volatile sink.

The models used for mantle simulations differ somewhat. One major difference is that NBS2012 include an approximation of dislocation creep (by dividing the activation energy by the power law index) but not plasticity, while we include plasticity but not dislocation creep. There are some other differences, such as our inclusion of composition-dependent phase transitions and the latent heat of melting (which does not appear in the equations presented in NBS2012). Different codes are also used (GAIA [*Hüttig and Stemmer*, 2008] rather than StagYY [*Armann and Tackley*, 2012; *Keller and Tackley*, 2009]), but this should not, in principle, affect the results. Their approach to atmospheric escape is also different, as NBS2012 used a simple exponential decrease as an approximation of the effects of escaping fluxes, while we focused on the actual processes involved and the modeling of mechanisms for both nonthermal escape and early hydrodynamic escape (which was not considered by NBS2012) and their evolution with time. Finally, the dependence of surface temperature on water content is not calculated in the same way. NBS2012 used published results by *Bullock and Grinspoon* [2001, Figure 6]. On the other hand, we self-consistently modeled the greenhouse effect in a simple way, using a method that does not take into account the complex mechanisms involved in cloud evolution that *Bullock and Grinspoon* [2001]describe. This approach leaves out some possible mechanisms and precision out but also relies less on hypothesis and is more adaptable for future developments and different conditions and planetary parameters.

The results obtained in the two studies also differ. While both indicate that atmosphere-mantle coupling results in stabilization of surface conditions, the physical mechanisms involved are different. NBS2012 suggested that when surface temperature increases enough (depending on the rheology) the surface becomes mobilized because the dislocation creep viscosity decreases. This causes resurfacing and heat loss, which cools the mantle and leads to lower activity and thus lower surface temperatures after some time. On the other hand, we observe that when temperature drops, a mobile lid regime akin to plate tectonics is favored, leading to higher activity. In our present models, we did not observe any large sudden increase in surface temperature from around 650 K to 850–900 K described by NBS2012, due to differences in how volatile fluxes are handled and the water concentration dependence of surface temperature.

Another, more subtle, difference between the two studies is their scope, as they complement each other. NBS2012 were mainly concerned about the effects of rheology on the coupled evolution of Venus.

The present work also considers rheology, but focuses more on the atmosphere, investigating the consequences the different processes and volatile fluxes have on long-term evolution and surface conditions, such as the range of possible atmosphere escape rates or their timing.

Our models presented here focus on the influence of the atmosphere on mantle convection and long-term evolution, including what is necessary to obtain realistic present-day conditions. As such, we based our mantle model on a case that was already shown to produce a reasonable mantle and crustal evolution for Venus [*Armann and Tackley*, 2012]. The model was indeed found to reproduce episodic behavior, mantle overturns, and generally fit observed characteristics of Venus (such as amplitudes of surface topography and geoid).

Considering the large number of parameters related to mantle and atmospheric treatments, a full test of their whole ranges is beyond what is possible in an initial paper. Nevertheless, it is indeed important to further study and verify if atmospheric coupling has similar effect for plausible mantle rheologies such as including dislocation creep (as in NBS2012) and a different crustal rheology, as well as the influence of volatiles. Those could modify significantly the response of the mantle to the surface temperature. It could further link the solid and fluid layers by highlighting the importance of volatile and water loss from the mantle both in terms of greenhouse effect in the atmosphere and rheology changes in the mantle.

Another improvement would be to include the possibility of recycling volatiles. The present simulations demonstrate a substantial amount of crustal and lithospheric recycling back into the deep mantle. This recycling exists both during stagnant lid times (by entrainment from the base) and episodic lid/plate tectonics (sinking slabs/lid overturn). To first order the effect could be small, as it would mainly stabilize the volatile content of the source of the melt, making it less likely to decrease drastically with time (an hypothesis we tested with different volatiles content evolution over time including constant concentrations). Recycling might also have implications for the mantle and, eventually, crustal rheology, which we will implement at some point. Additionally, it suggests another mode of atmosphere-interior coupling. Furthermore, accounting for the fact that a large fraction of magmatism may be intrusive rather than extrusive could have a major effect both on lithospheric dynamics (producing a hot, weak crust/lithosphere, as in *Tackley and Armann* [2013]) and on volatile cycling, greatly reducing volatile degassing.

Finally, partitioning of trace elements into the melt and hence crust could be accounted for [*Xie and Tackley*, 2004], allowing a study of ^{40}Ar outgassing and crustal trace element concentrations. Recent results [*Armann and Tackley*, 2012] obtained a range of crustal heat-producing element concentrations consistent with measurements by the Venera and Vega landers.

4.6. Habitability?

Our simulations indicate that processes leading to Venus' present state are not as exotic as sometimes suggested, but are, on the contrary, very similar to what could have occurred on Earth given different initial parameters. A form of plate tectonics could have taken place. Two main differences are the apparent relative dryness of Venus compared to the Earth and the fact that CO_2 seems to be located in the atmosphere, while on Earth it has been buried. Both are directly linked to the question of surface temperatures. With a volatile-depleted mantle, it is unlikely that atmospheric CO_2 pressure would change much during the late evolution. It is then difficult to reduce surface temperature below 500–550 K, and even then, that would correspond to a case where water is lost almost completely. Under those conditions, it is dubious that habitable conditions can be sustained.

Indeed, while it is possible to get water to condense at high temperatures (like 650 K) provided surface pressure is high enough (as it should be on Venus), reaching such low temperatures with current conditions might mean that most, if not all, of the water has been removed from Venus' atmosphere as early as around the end of the magma ocean [*Hamano et al*., 2013; *Lebrun et al*., 2013]. Likewise, effects from other species, at the current state of our knowledge, would be unlikely to allow for a large enough temperature drop (see *Bullock and Grinspoon* [2001] for the effect of SO_2, for example).

If, under early Venus-like (or perhaps primitive Earth) conditions, temperatures could have been lower with water still present (with a thinner CO_2 atmosphere, for example, or different conditions in the atmosphere, involving clouds and other species not used here), we show that plate tectonics could have occurred. Plate

tectonics is thought to be the main process on Earth that recycles CO_2 into the solid planet. This, in turn, could have prevented the onset of the large greenhouse effect due to CO_2 and stabilized the climate of the planet on a more Earth-like level.

As observed in our current model, however, this is unlikely to take place during the last 4 Gyr or so. Two possibilities exist. We might be neglecting an important mechanism, which would probably be the recycling of surface material into the mantle. Or, the fate of habitability might be decided early in the history of terrestrial bodies.

Gillmann et al. [2009] proposed a self-consistent model for the evolution of early Venus based on isotopic data and thermal atmospheric escape modeling. They proposed that hydrodynamic escape efficiently pumped water out of the atmosphere and mantle of Venus while the magma ocean still existed and left the planet dry. CO_2 accumulated in the atmosphere when the magma ocean froze and accounted for later high surface temperatures. Earth would be different in the larger amount of water it received and the smaller hydrodynamic escape, meaning some water would be left on the planet when the magma ocean froze.

It therefore seems that eventual habitability and long-term surface conditions might be decided during a short window of opportunity that depends on three characteristics of the planet: (i) initial volatile endowment, (ii) atmospheric escape flux, and (iii) degassing rate (of CO_2, here). The cooling rate of the surface is governed by these factors. If they adjust in a way that allows for the temperature to drop while water still exists on the planet, then a long-term stabilizing effect can be put in place and sustain itself: the planet is cool enough that water vapor does not add to the greenhouse effect, and it allows plate tectonics to bury CO_2, which does not accumulate in the atmosphere. Other cases result in Venus-like situations: too large escape fluxes remove most of the water, and then CO_2 accumulates in the atmosphere, while lower escape would probably prevent surface temperatures to drop fast enough to allow this "cold window."

The timing of the different events is likely to play an important role in this evolution. Among other paths, large impacts may deeply modify early conditions. Not only could they remove a large part of the atmosphere, potentially creating part of the "cold window" we mentioned, but they are also a source of volatiles that could bring large amount of water to early planetary bodies.

5. Conclusions

Here we have presented a model for the coupling of the atmosphere and interior processes of Venus. The model includes tracking of volatile fluxes, a fully dynamical mantle convection calculation, and changing surface temperature. The mantle simulations use the StagYY model [*Tackley*, 2008] which includes melting, volcanism, phase transitions, radiogenic heating, realistic rheology, and plastic yielding. The atmospheric treatment is based on a 1-D radiative-convective gray atmosphere model with water and CO_2 as greenhouse gases. Atmospheric losses are computed by modeling the early linked hydrodynamic escape of oxygen and hydrogen and computing of a history of late nonthermal escape through the whole evolution of the planet.

Our main conclusions are as follows:

1. Using sets of parameters that are consistent with best estimates for Venus' characteristics, this work finds a set of possible evolution histories that result in present-day surface conditions consistent with observations of Venus, in terms of atmospheric CO_2 pressure, water content, and surface temperature.
2. Computed evolution histories of atmospheric CO_2 and H_2O show that surface temperature varies mainly with water content. Water was removed efficiently from the atmosphere early on but can accumulate to the present-day value during the later stages in which removal is less efficient, even with low water concentration in magma. CO_2 pressure does not vary much over the history of Venus after the initial events and end of the accretion—we observe a rise in CO_2 pressure of less than 0.5% in most cases when a reduced mantle is considered. It is unlikely that Venus' CO_2 atmosphere was built over the course of several massive degassing (resurfacing) events; instead, most of the CO_2 was in the atmosphere since the end of the magma ocean phase. However, if Venus' mantle is oxidized and the lavas rich in CO_2 (1%(w.)) a moderate buildup of several bars over the history is possible.
3. The effect of the atmosphere-mantle coupling is to stabilize the surface conditions of Venus. The atmospheric water content varies less in the coupled models than in the uncoupled ones, in particular, in the late evolution, which translates into a more stable surface temperature on the long term.

4. Hydrodynamic escape ensures that 4.5 Ga ago, the atmosphere of Venus is likely to have lost most of its initial endowment of water (barring the case of a huge initial water content of several tens of terrestrial ocean equivalents or more). This means that the "hot" stage of early Venus could have been short (several tens of Myr). Incidentally, realistic present-day surface temperatures require that the initial water content should be mainly lost (typically, the models need no more water than can be removed in 2 Gyr), a condition massive hydrodynamic escape can help fulfill.
5. Late nonthermal escape intensities that lead to the correct present-day surface temperature cover a limited range of values (much less than the present-day uncertainty in models and observation).
6. Present-day surface temperature is mainly determined by late nonthermal escape in our models. It also depends, in part, on the strength of degassing and thus on the water content of the magmas and mechanisms of degassing, which are difficult to constrain. For the lower concentrations used here, degassing appears to be secondary.
7. Our results produce a realistic late-stage (last 1 Gyr) volcanic activity, in line with recent discovery of present-day volcanism on Venus. It features resurfacing events, in the form of mantle overturns and in most models, late activity with at least one large event during the last billion years possibly explaining the young age of Venusian crust. Additionally, volcanic production rates are also consistent with estimates of Venus' evolution since the last resurfacing event and indicative of an active planet.
8. Our simulations evidence a clear feedback between surface temperature and mantle convection. Temperature decreases lead to the mobile lid (plate tectonic-like) convection mode with an increased magma production rate. On the other hand, a warmer surface favors the stagnant lid mode, with a resulting decrease in volcanic activity and degassing. This feedback tends to stabilize Venus' climate further.
9. The mantle convection mode in coupled simulations displays a more chaotic variation than in uncoupled (constant surface temperature) simulations. Quiescent periods do not have a characteristic length and a general overall decrease in activity is not always obvious. This further reinforces the importance of surface temperature on mantle convection.
10. In our preferred model, plate tectonics occurred on early Venus (during a period of relatively low surface temperature) and stopped around 3 Gyr ago to be replaced by stagnant lid convection. This regime lasted around 1 Gyr before it was replaced by episodic lid convection 2 Gyr ago. This regime would still be in place at present-day and responsible for the state of present-day surface conditions and recent resurfacing.

Acknowledgments

C. Gillmann was supported by an ETH Fellowship. The final stages of the study were done at the Royal Observatory of Belgium with funding by the Interuniversity Attraction Pole Program initiated by the Belgian Science Policy Office. We thank an anonymous reviewer and Mark Bullock for their insightful comments, which helped in improving the manuscript. Details on how the data used for this article are available in the main text.

References

Abe, Y., and T. Matsui (1988), Evolution of an impact-generated H2O-CO2 atmosphere and formation of a hot proto-ocean on Earth, *J. Atmos. Sci.*, *45*, 3081–3101.

Ahrens, T. J., (1981). Carbon dioxide within Venus and the Earth. *Adv. Space Rae.*, *1*, 177—187.

Ahrens, T. J. (1993), Impact erosion of terrestrial planetary atmospheres, *Annu. Rev. Earth Planet. Sci.*, *21*, 525–555.

Anderson, F., and S. Smrekar (1999), *Tectonic Effects of Climate Change on Venus*. Journal of Geophysical Research, *104*(E12), 30,743–30,756, doi:10.1029/1999JE001082.

Armann, M., and P. J. Tackley (2012), Simulating the thermochemical magmatic and tectonic evolution of Venus's mantle and lithosphere: Two-dimensional models, *J. Geophys. Res.*, *117*, E12003, doi:10.1029/2012JE004231.

Arvidson, R. E., R. Greeley, M. C. Malin, R. S. Saunders, N. Izemberg, J. J. Plaut, E. R. Stofan, and M. K. Shepard (1992), Surface modification of Venus as inferred from Magella, observations of plains, *J. Geophys. Res.*, *97*(E8), 13,303–13,317, doi:10.1029/92JE01384.

Barabash, S., et al. (2007), The Analyser of Space Plasmas and Energetic Atoms (ASPERA-4) for the Venus Express mission, *Planet. Space Sci.*, *55*(12), 1772–1792.

Bauer, S. J., and H. Lammer (2004), *Planetary Aeronomy: Atmosphere Environments in Planetary Atmospheres*, Springer, Berlin, Heidelberg, New York.

Brace, L. H., R. F. Theis, and W. R. Hoegy (1987), Ionospheric electron temperature at solar maximum, *Adv. Space Res.*, *7*(6), 99–106.

Bullock, M. A., D. H. Grinspoon, and J. W. Head, (1993a), Venus resurfacing rates: Constraints provided by 3-D Monte Carlo simulations. Lunar and Planetary Inst., Twenty-fourth Lunar and Planetary Science Conference. Part 1: A-F p 213–214 (SEE N94-12015 01–91).

Bullock, M. A., D. H. Grinspoon, and J. W. Head (1993b), Venus resurfacing rates: Constraints provided by 3-D Monte Carlo simulations, *Geophys. Res. Lett.*, *20*, 2147–2150, doi:10.1029/93GL02505.

Bullock, M. A., and D. H. Grinspoon (1996), The stability of climate on Venus, *J. Geophys. Res.*, *101*, 7521–7529, doi:10.1029/95JE03862.

Bullock, M. A., and D. H. Grinspoon (2001), The recent evolution of climate on Venus, *Icarus*, *150*, 19–37.

Bullock, M. A., and D. H. Grinspoon (2003), Did Venus Experience One Great Transition or Two?, in *American Astronomical Society*, Bull. Am. Astron. Soc., DPS meeting #35, #44.03, vol. 35, p. 1007.

Burton, M. R., G. M. Sawyer, and D. Granieri (2013), Introduction: Volcanic CO2 emissions in the geological carbon cycle, *Rev. Mineral. Geochem.*, *75*, 323–354.

Chassefière, E. (1996a), Hydrodynamic escape of oxygen from primitive atmospheres: Applications to the cases of Venus and Mars, *Icarus*, *124*, 537–552.

Chassefière, E. (1996b), Hydrodynamic escape of hydrogen from a hot water-rich atmosphere: The case of Venus, *J. Geophys. Res.*, *101*, 26,039–26,056, doi:10.1029/96JE01951.

Chassefière, E., and F. Leblanc (2004), Mars atmospheric escape and evolution: Interaction with the solar wind, *Planet. Space Sci.*, *52*, 1039–1058.
Crisp, J. A. (1984), Rates of magma emplacement and volcanic output, *J. Volc. Geotherm. Res.*, *20*, 177–211.
Debaille, V., A. D. Brandon, Q. Y. Yin, and B. Jacobsen (2007), Coupled 142Nd–143Nd evidence for a protracted magma ocean in Mars, *Nature*, *450*, 525–528.
de Bergh, C., et al. (1995), Water in the deep atmosphere of Venus from high resolution spectra of the night side, *Adv. Space Res.*, *15*(4), 79–88.
de Niem, D., E. Kührt, A. Morbidelli, and U. Motschumann (2012), Atmospheric erosion and replenishment induced by impacts upon the Earth and Mars during a heavy bombardment, *Icarus*, *221*(2), 495–507.
Donahue, T. M. (1999), New analysis of hydrogen and deuterium escape from Venus, *Icarus*, *141*(2), 226–235.
Elkins-Tanton, L. T., S. E. Smrekar, P. C. Hess, and E. M. Parmentier (2007), Volcanism and volatile recycling on a one-plate planet: Applications to Venus, *J. Geophys. Res.*, *112*, E04S06, doi:10.1029/2006JE002793.
Elkins-Tanton, L. T. (2008), Linked magma ocean solidification and atmospheric growth for Earth and Mars, *Earth Planet. Sci. Lett.*, *271*, 181–191.
Esposito, L. W., R. G. Knollenberg, M. Y. A. Marov, O. B. Toon, and R. P. Turco (1983), The clouds and Hazes of Venus, in *Venus*, edited by D. M. Hunten et al., pp. 484, University of Arizona Press, Tucson, Ariz.
Fedorov, A., S. Barabash, J.-A. Sauvaud, Y. Futaana, T. L. Zhang, R. Lundin, and C. Ferrier (2011), Measurements of the ion escape rates from Venus for solar minimum, *J. Geophys. Res.*, *116*, A07220, doi:10.1029/2011JA016427.
Fegley, B., and R. G. Prinn (1989), Estimation of the rate of volcanism on Venus from reaction rate measurements, *Nature*, *337*, 55–58.
Fowler, A. C., and S. B. G. O'Brian (1996), A mechanism for episodic subduction on Venus, *J. Geophys. Res.*, *101*(E2), 4755–4763, doi:10.1029/95JE03261.
Gerya, T. V. (2014), Plume-induced crustal convection: 3D thermomechanical model and implications for the origin of novae and coronae on Venus, *Earth Planet. Sci. Lett.*, *391*, 183–192, doi:10.1016/j.epsl.2014.02.005.
Gillmann, C., E. Chassefière, and P. Lognonné (2009), A consistent picture of early hydrodynamic escape of Venus atmosphere explaining present Ne and Ar isotopic ratios and low oxygen atmospheric content, *Earth and Plant. Sci. Lett.*, *286*, 503–513, doi:10.1016/j.epsl.2009.07.016.
Gislason, S. R., À. Snorrason, H. K. Kristmannsdòttir, À. E. Sveinbjörnsdòttir, P. Torsander, J. Òlafsson, S. Castet, and B. Dupre (2002), Effects of volcanic eruptions on the CO2 content of the atmosphere and the oceans: The 1996 eruption and flood within the Vatnajökull Glacier, Iceland, *Chem. Geol.*, *190*(2002), 181–205.
Golabek, G. J., T. Keller, T. V. Gerya, G. Zhu, P. J. Tackley, and J. A. D. Connolly (2011), Origin of the Martian dichotomy and Tharsis from a giant impact causing massive magmatism, *Icarus*, *215*(1), 346–357.
Gough, D. O. (1981), Solar interior structure and luminosity variations, *Solar Phys.*, *74*, 21–34.
Greeley, R., and B. D. Schneid (1991), Magma generation on Mars: Amounts, rates, and comparisons with Earth, Moon, and Venus, *Science*, *254*, 996–998.
Grinspoon, D. H. (1993), Implications of the high D/H ratio for the sources of water in Venus' atmosphere, *Nature*, *363*, 428–431.
Grott, M., A. Morschhauser, D. Breuer, and E. Hauber (2011), Volcanic outgassing of CO2 and H2O on Mars, *Earth Planet. Sci. Lett.*, *308*, 391–400.
Hamano, K., Y. Abe, and H. Genda (2013), Emergence of two types of terrestrial planet on solidification of magma ocean, *Nature*, *497*, 607–610.
Hauck, S. A., R. J. Phillips, and M. H. Price (1998), Venus: Crater distribution and plains resurfacing models (1991–2012), *J. Geophys. Res.*, *103*(E6), 13,635–13,642, doi:10.1029/98JE00400.
Head, J. W., and L. Wilson (2003), Deep submarine pyroclastic eruptions: Theory and predicted landforms and deposits, *J. Volcanol. Geotherm. Res.*, *121*, 155–193.
Hernlund, J. W., and P. Tackley (2008), Modeling mantle convection in the spherical annulus, *Phys. Earth Planet. Int.*, *171*(1–4), 48–54.
Herrick, R. R. (1994), Resurfacing history of Venus, *Geology*, *22*(8), 703–706.
Hirschmann, M. M., and A. C. Withers (2008), Ventilation of CO2 from a reduced mantle and consequences for the early Martian greenhouse, *Earth Planet. Sci. Lett.*, *270*, 147–155.
Hodges, R. R., Jr. (2000), Distributions of hot oxygen for Venus and Mars, *J. Geophys. Res.*, *105*, 6971–6981, doi:10.1029/1999JE001138.
Hunten, D., R. Pepin, and J. Walker (1987), Mass fractionation in hydrodynamic escape (of gases from planetary atmospheres), *Icarus*, *69*, 532–549.
Hüttig, C., and K. Stemmer (2008), Finite volume discretization for dynamic viscosities on Voronoi grids, *Phys. Earth Planet. Int.*, *171*, 137–146.
Irifune, T., and A. E. Ringwood (1993), Phase-transformations in subducted oceanic-crust and buoyancy relationships at depths of 600–800 km in the mantle, *Earth Planet. Sci. Lett.*, *117*(1–2), 101–110.
Ivanov, M. A., and J. W. Head (1996), Tessera terrain in Ovda Regio, Venus: Preliminary results of a geologic mapping traverse, In Lunar and Planetary Institute Science Conference Abstracts, vol. 27, p. 591.
Jakosky, B. M., R. O. Pepin, R. E. Johnson, and J. L. Fox (1994), Mars atmospheric loss and isotopic fractionation by solar-wind induced sputtering and photochemical escape, *Icarus*, *111*, 271–288.
Janle, P., A. T. Basilevsky, M. A. Kreslavsky, and E. N. Slyuta (1992), Heat-loss and tectonic style of Venus, *Earth Moon Planets*, *58*(1), 1–29.
Jarvinen, R., E. Kallio, P. Janhunen, S. Barabash, T. L. Zhang, V. Pohjola, and I. Sillanpää (2009), Oxygen ion escape from Venus in a global hybrid simulation: Role of the ionospheric O^+ ions, *Ann. Geophys.*, *27*, 4333–4348.
Kallio, E., R. Jarvinena, and P. Janhunen (2006), Venus–solar wind interaction: Asymmetries and the escape of O^+ ions, *Planet. Space Sci.*, *54*(2006), 1472–1481.
Karato, S., and P. Wu (1993), Rheology of the upper mantle—A synthesis, *Science*, *260*(5109), 771–778.
Kasting, J. F., and J. B. Pollack (1983), Loss of water from Venus. I. Hydrodynamic escape of hydrogen, *Icarus*, *53*, 479–508.
Kasting, J. F., J. B. Pollack, and T. P. Ackerman (1984), Response of Earth's atmosphere to increases in solar flux and implications for loss of water from Venus, *Icarus*, *57*, 335–355.
Kasting, J. F. (1988), Runaway and moist greenhouse atmospheres and the evolution of Earth and Venus, *Icarus*, *74*, 472–494.
Kasting, J. F., and D. Catling (2003), Evolution of a habitable planet, *Ann. Rev. Astron. Astrophys.*, *41*, 429–463.
Kaula, W. M. (1999), Constraints on Venus evolution from radiogenic Argon, *Icarus*, *139*(1), 32–39.
Keller, T., and P. J. Tackley (2009), Towards self-consistent modelling of the Martian dichotomy: The influence of low-degree convection on crustal thickness distribution, *Icarus*, *202*(2), 429–443.
Kiefer, W. S. (2003), Melting on the Martian mantle: Shergottite formation and implications for present-day mantle convection on Mars, *Meteorit. Planet. Sci.*, *38*, 1815–1832.

Kohlstedt, D. L., B. Evans, and S. J. Mackwell (1995), Strength of the lithosphere—Constraints imposed by laboratory experiments, *J. Geophys. Res.*, *100*(B9), 17,587–17,602, doi:10.1029/95JB01460.
Kulikov, Y. N., et al. (2006), Atmospheric and water loss from early Venus, *Planet. Space Sci.*, *54*, 1425–1444.
Lammer, H., H. I. M. Lichtenegger, C. Kolb, I. Ribas, E. F. Guinan, R. Abart, and S. J. Bauer (2003a), Loss of water from Mars: Implications for the oxidation of the soil, *Icarus*, *106*, 9–25.
Lammer, H., F. Selsis, I. Ribas, E. F. Guinan, S. J. Bauer, and W. W. Weiss (2003b), Atmospheric loss of exoplanets resulting from stellar X-ray and extreme ultraviolet heating, *Astrophys. J.*, *598*, L121–L124.
Lammer, H., et al. (2006), Loss of hydrogen and oxygen from the upper atmosphere of Venus. *Planet. Space Sci.*, doi:10.1016/j.pss.2006.04.022, in press.
Lebrun, T., H. Massol, E. Chassefiere, A. Davaille, E. Marcq, P. Sarda, F. Leblanc, and G. Brandeis (2013), Thermal evolution of an early magma ocean in interaction with the atmosphere, *J. Geophys. Res. Planets*, *118*, 1155–1176, doi:10.1002/jgre.20068.
Lenardic, A., A. M. Jellinek, and L.-N. Moresi (2008), A climate induced transition in the tectonic style of a terrestrial planet, *Earth Planet. Sci. Lett.*, *271*, 34–42.
Lopez, I., R. Oyarzun, A. Marquez, F. Doblas-Reyes, and A. Lorrieta (1999), Progressive build up of CO_2 in the atmosphere of Venus through multiple volcanic resurfacing events, *Earth Moon Planets*, *81*, 187–192.
Luhmann, J. G., and J. U. Kozyra (1991), Dayside pickup oxygen ion precipitation at Venus and Mars: Spatial distributions, energy deposition and consequences, *J. Geophys. Res.*, *96*, 5457–5467, doi:10.1029/90JA01753.
Luhmann, J. G. (1993), A model of the ionospheric tail rays of Venus, *J. Geophys. Res.*, *98*, 17,615–17,621, doi:10.1029/93JA01471.
Lundin, R., and S. Barabash (2004), Evolution of the Martian atmosphere and hydrosphere: Solar wind erosion studied by ASPERA-3 on Mars Express, *Planet. Space Sci.*, *52*, 1059–1071.
Marcq, E. (2012), A simple 1-D radiative-convective atmospheric model designed for integration into coupled models of magma ocean planets (1991–2012), *J. Geophys. Res.*, *117*, EO1001, doi:10.1029/2011JE003912.
Matsui, T., and E. Tajika, (1995). Comparative study of crustal production rates of Mars, Venus and the Earth. Abstracts of the Lunar and Planetary Science Conference, volume 26, 909 pp.
McComas, D. J., H. E. Spence, C. T. Russell, and M. A. Saunders (1986), The average magnetic field draping and consistent plasma properties of the Venus magnetotail, *J. Geophys. Res.*, *91*(A7), 7939–7953, doi:10.1029/JA091iA07p07939.
McKinnon, W. B., K. J. Zhanle, B. A. Ivanov, and J. H. Melosh (1997), Cratering on Venus: Models and observations, in *Venus II*, pp. 969–1014, Arizona Univ. Press, Tucson.
Moore, K. R., V. A. Thomas, and D. J. McComas (1991), Global hybrid simulation of the solar wind interaction with the dayside of Venus, *J. Geophys. Res.*, *96*, 7779–7791, doi:10.1029/91JA00013.
Moresi, L.-N., and V. S. Solomatov (1998), Mantle convection with a brittle lithosphere: Thoughts on the global tectonic style of the Earth and Venus, *Geophys. J. Int.*, *133*, 669–682.
Morschhauser, A., M. Grott and D. Breuer (2009), Mantle degassing and the origin of the Venusian atmosphere. EPSC Abstracts, vol. 4, EPSC2009, 2009 European Planetary Science Congress.
Nakagawa, T., and P. J. Tackley (2004), Effects of thermo-chemical mantle convection on the thermal evolution of the Earth's core, *Earth Planet. Sci. Lett.*, *220*, 107–119.
Nakagawa, T., and P. J. Tackley (2005), The interaction between the post-perovskite phase change and a thermo-chemical boundary layer near the core-mantle boundary, *Earth Planet. Sci. Lett.*, *238*, 204–216.
Nakagawa, T., and P. J. Tackley (2010), Influence of initial CMB temperature and other parameters on the thermal evolution of Earth's core resulting from thermo-chemical spherical mantle convection, *Geophys. Geochem. Geosyst.*, *11*(Q06001), doi:10.1029/2010GC003031.
Nakagawa, T., P. J. Tackley, F. Deschamps, and J. A. D. Connolly (2009), Incorporating self-consistently calculated mineral physics into thermo-chemical mantle convection simulations in a 3D spherical shell and its influence on seismic anomalies in Earth's mantle, *Geochem. Geophys. Geosyst*, *10*, Q03004, doi:10.1029/2008GC002280.
Nakagawa, T., P. J. Tackley, F. Deschamps, and J. A. D. Connolly (2010), The influence of MORB and harzburgite composition on thermo-chemical mantle convection in a 3-D spherical shell with self-consistently calculated mineral physics, *Earth Planet. Sci. Lett.*, *296*, 403–412.
Namiki, N., and S. C. Solomon (1998), Volcanic degassing of argon and helium and the history of crustal production on Venus, *J. Geophys. Res.*, *103*, 3655–3678, doi:10.1029/97JE03032.
Nimmo, F., and D. P. McKenzie (1997), Convective thermal evolution of the upper mantles of Earth and Venus, *Geophys. Res. Lett.*, *24*(12), 1539–1543, doi:10.1029/97GL01382.
Nimmo, F., and D. McKenzie (1998), Volcanism and tectonics on Venus, *Annu. Rev. Earth Planet. Sci.*, *26*, 23–51.
Noack, L., D. Breuer, and T. Spohn (2012), Coupling the atmosphere with interior dynamics: Implications for the resurfacing of Venus, *Icarus*, *217*, 484–498, doi:10.1016/j.icarus.2011.08.026.
O'Brien, D. P., A. Morbidelli, and H. F. Levison (2006), Terrestrial planet formation with strong dynamical friction, *Icarus*, *184*, 39–58.
Ono, S., E. Ito, and T. Katsura (2001), Mineralogy of subducted basaltic crust (MORB) from 25 to 37 GPa, and chemical heterogeneity of the lower mantle, *Earth Planet. Sci. Lett.*, *190*(1–2), 57–63.
Parmentier, E. M., and P. C. Hess (1992), Chemical dieferentiation of a convecting planetary interior: Consequences for a one plate planet such as Venus, *Geophys. Res. Lett.*, *19*(20), 2015–2018, doi:10.1029/92GL01862.
Phillips, R. J., et al. (1992), Impact craters and Venus resurfacing history, *J. Geophys. Res.*, *97*, 15,923–15,948, doi:10.1029/92JE01696.
Phillips, R. J., and V. L. Hansen (1998), Geological evolution of Venus: Rises, plains, plumes, and plateaus, *Science*, *279*, 1492–1497.
Phillips, R. J., M. A. Bullock, and S. A. Hauck II (2001), Climate and interior coupled evolution on Venus, *Geophys. Res. Lett.*, *28*(9), 1779–1782, doi:10.1029/2000GL011821.
Pollack, J. B., O. B. Toon, and R. Boese (1980), Greenhouse models of Venus' high surface temperature, as constrained by Pioneer Venus measurements, *Geophys. Res. Lett.*, *85*(A13), 8223–8231, doi:10.1029/JA085iA13p08223.
Price, M., and J. Suppe (1994), Mean age of rifting and volcanism on Venus deduced from impact crater densities, *Nature*, *372*, 756–759.
Raymond, S. N., T. Quinn, and J. I. Lunine (2006), High-resolution simulations of the final assembly of Earth-like planets. I. Terrestrial accretion and dynamics, *Icarus*, *183*, 265–282.
Reese, C. C., V. S. Solomatov, and C. P. Orth (2007), Mechanisms for cessation of magmatic resurfacing on Venus, *J. Geophys. Res.*, *112*, E04S04, doi:10.1029/2006JE002782.
Ribas, I., E. F. Guinan, M. Güdel, and M. Audard (2005), Evolution of the solar activity over time and effects on planetary atmospheres. I. High-energy irradiances (1–1700 Å), *Astrphys. J.*, *622*, 680–694.
Ribas, I., G. F. Porto de Mello, L. D. Ferreira, E. Hébrard, F. Selsis, S. Catalán, A. Garcés, J. D. do Nascimento Jr., and J. R. de Medeiros (2010), Evolution of the solar activity over time and effects on planetary atmospheres. II. κ1 Ceti, an analog of the Sun when life arose on Earth, *Astrophys. J.*, *714*, 384, doi:10.1088/0004-637X/714/1/384.

Robinson, T. D., and D. C. Catling (2012), An analytic radiative-convective model for planetary atmospheres, *Astrophys. J.*, *757*(10), 104.
Romeo, I., and D. L. Turcotte (2010), Resurfacing on Venus, *Planet. Space Sci.*, *58*, 1374–1380.
Ruedas, T., P. J. Tackley, and S. C. Solomon (2013a), Thermal and compositional evolution of the Martian mantle: Effects of phase transitions and melting, *Phys. Earth Planet. Inter.*, *216*, 32–58.
Ruedas, T., P. J. Tackley, and S. C. Solomon (2013b), Thermal and compositional evolution of the Martian mantle: Effects of water, *Phys. Earth Planet. Inter.*, *220*, 50–72.
Saito, T., N. Ishikawa, and H. Kamata (2007), Magnetic petrology of the 1991–1995 dacite lava of Unzen volcano, Japan: Degree of oxidation and implications for the growth of lava domes, *J. Volcanol. Geotherm. Res.*, *164*, 268–283.
Schaber, G. G., et al. (1992), Geology and distribution of impact craters on Venus: What are they telling us?, *J. Geophys. Res.*, *97*(E8), 13,257–13,301, doi:10.1029/92JE01246.
Schubert, G., S. Solomatov, P. J. Tackley, and D. L. Turcotte (1997), Mantle convection and the thermal evolution of Venus, in *Venus II. Geology, Geophysics, Atmosphere, and Solar Wind Environment*, pp. 1245–1288, Univ. of Arizona Press, Tucson, Ariz.
Schubert, G., D. L. Turcotte, and P. Olson (2001), *Mantle Convection in the Earth and Planets*, Cambridge Univ. Press, Cambridge.
Shaligyn, E. V., W. J. Markiewicz, A. T. Basilevsky, D. V. Titov, N. I. Ignatiev, and J. W. Head (2014), Bright transient spots in Ganiki Chasma, Venus. Lunar and Planetary Institute Conference Abstracts, 2556.
Shuvalov, V. (2009), Atmospheric erosion induced by oblique impacts, *Meteorit. Planet. Sci.*, *44*(8), 1095–1105.
Smith, D. S., J. Scalo, and J. G. Wheeler (2004), Transport of ionizing radiation in terrestrial-like exoplanet atmospheres, *Icarus*, *171*, 229–253.
Smolarkiewicz, P. K. (1984), A fully multidimensional positive definite advection transport algorithm with small implicit diffusion, *J. Comp. Phys.*, *54*(2), 325–362.
Smrekar, S. E., E. R. Stofan, N. Mueller, A. Treiman, L. Elkins-Tanton, J. Helbert, G. Piccioni, and P. Drossart (2010), Recent hotspot volcanism on Venus from VIRTIS emissivity data, *Science*, *328*(5978), 605–608.
Solomon, S. C., M. A. Bullock, and D. H. Grinspoon (1999), Climate change as a regulator of tectonics on Venus, *Science*, *286*, 87–90.
Strom, R. G., G. G. Schaber, and D. D. Dawson (1993), The global resurfacing of Venus, *Bull. Am. Astron. Soc.*, *25*, 1084.
Strom, R. G., G. G. Schaber, and D. D. Dawson (1994), The global resurfacing of Venus, *J. Geophys. Res.*, *99*, 10,899–10,926.
Tackley, P. J. (1993), Effects of strongly temperature-dependent viscosity on time-dependent, 3-dimensional models of mantle convection, *Geophys. Res. Lett.*, *20*(20), 2187–2190, doi:10.1029/93GL02317.
Tackley, P. J. (1996), Effects of strongly variable viscosity on three-dimensional compressible convection in planetary mantles, *J. Geophys. Res.*, *101*, 3311–3332, doi:10.1029/95JB03211.
Tackley, P. J. (1998), Three-dimensional simulations of mantle convection with a thermochemical CMB boundary layer: D"?, in *The Core-Mantle Boundary Region*, edited by M. Gurnis et al., pp. 231–253, AGU, Washington, D. C.
Tackley, P. J. (2000a), Self-consistent generation of tectonic plates in time-dependent, three-dimensional mantle convection simulations Part 1: Pseudo-plastic yielding, *Geochem., Geophys., Geosys.*, *1*, Paper number 2000GC000036.
Tackley, P. J. (2000b), Self-consistent generation of tectonic plates in time-dependent, three-dimensional mantle convection simulations Part 2: Strain weakening and asthenosphere, *Geochem., Geophys., Geosyst.*, *1*, Paper number 2000GC000043.
Tackley, P. J., and S. D. King (2003), Testing the tracer ratio method for modeling active compositional fields in mantle convection simulations, *Geochem. Geophys. Geosyst.*, *4*(4), 8302, doi:10.1029/2001GC000214.
Tackley, P. J. (2008), Modelling compressible mantle convection with large viscosity contrasts in a three-dimensional spherical shell using the yin-yang grid, *Phys. Earth Planet. Int.*, *171*, 7–18, doi:10.1016/j.pepi.2008.08.005.
Tackley, P. J., and M. Armann (2013), Simulating the thermochemical magmatic and tectonic evolution of Venus's mantle and lithosphere: Intrusive vs. extrusive magmatism, Abstract EGU2013-13743, EGU Spring Meeting.
Taylor, F., and D. Grinspoon (2009), Climate evolution of Venus, *J. Geophys. Res.*, *114*, E00B40, doi:10.1029/2008JE003316.
Terada, N., S. Machida, and H. Shinagawa (2002), Global hybrid simulation of the Kelvin-Helmholtz instability at the Venus ionopause. *J. Geophys. Res.*. *107*(A12), 1471, doi:10.1029/2001JA009224.
Tian, F., J. F. Kasting, H. Liu, and R. G. Roble (2008), Hydrodynamic planetary thermosphere model: 1. Response of the Earth's thermosphere to extreme solar EUV conditions and the significance of adiabatic cooling, *J. Geophys. Res.*, *113*(E05008), doi:10.1029/2007JE002946.
Trompert, R. A., and U. Hansen (1998), On the Rayleigh number dependence of convection with a strongly temperature-dependent viscosity, *Phys. Fluids*, *10*, 351.
Turcotte, D. L. (1993), An episodic hypothesis for Venusian tectonics, *J. Geophys. Res.*, *98*(E9), 17,061–17,068, doi:10.1029/93JE01775.
Turcotte, D. L. (1995), How does Venus lose heat?, *J. Geophys. Res.*, *100*(E8), 16,931–16,940, doi:10.1029/95JE01621.
Turcotte, D. L., G. Morein, D. Roberts, and B. D. Malamud (1999), Catastrophic resurfacing and episodic subduction on Venus, *Icarus, 139*(1), 49–54.
Volkov, V. P., and M. Y. Frenkel (1993), The modeling of Venus' degassing in terms of K-Ar system, *Earth Moon Planets*, *62*(2), 117–129.
Wendlandt, R. F. (1991), Oxygen diffusion in basalt and andesite melts: Experimental results and discussion of chemical versus tracer diffusion, *Contrib. Mineral. Petrol.*, *198*, 463–471.
Xie, S., and P. J. Tackley (2004), Evolution of helium and argon isotopes in a convecting mantle, *Phys. Earth Planet. Inter.*, *146*(3–4), 417–439.
Xu, W., C. Lithgow-Bertelloni, L. Stixrude, and J. Ritsema (2008), The effect of bulk composition and temperature on mantle seismic structure, *Earth Planet. Sci. Lett.*, *275*(1–2), 70–79.
Yamazaki, D., and S. Karato (2001), Some mineral physics constraints on the rheology and geothermal structure of Earth's lower mantle, *Amer. Mineral.*, *86*(4), 385–391.
Zahnle, K. J., and J. F. Kasting (1986), Mass fractionation during transonic escape and implications for loss of water from Mars and Venus, *Icarus*, *68*, 462–480.
Zhang, M. H. G., J. G. Luhmann, S. W. Bougher, and A. F. Nagy (1993), The ancient oxygen atmosphere of Mars: Implications for atmosphere evolution, *J. Geophys. Res.*, *98*, 10,915–10,923, doi:10.1029/93JE00231.
Zolotov, M. Y., and V. P. Volkov (1992), Chemical processes on the planetary surface, in *Venus Geology, Geochemistry, and Geophysics: Research Results From USSR*, edited by V. L. Barsukov Sr., pp. 177–199, Ariz. Univ. Press.
Zolotov, M. Y. (1996), A model of the Venus atmosphere evolution along with titanhematite-magnetite-pyrite buffer. Abstracts of the Lunar and Planetary Science Conference, vol. 26, 1569 pp., (1995).